Decoding the linear viscoelastic properties of model telechelic metallo-supramolecular polymers

Flanco Zhuge,[a] Laurence G. D. Hawke, Charles-Andre Fustin,[b] Jean-Francois Gohy,[c] and Evelyne van Ruymbeke[d]

Institute of Condensed Matter and Nanosciences (IMCN), Bio and Soft Matter Division (BSMA), Université catholique de Louvain, Croix du Sud 1 & Place L. Pasteur 1, B-1348 Louvain-la-Neuve, Belgium

(Received 8 May 2017; final revision received 28 June 2017; published 1 November 2017)

Abstract

This work focuses on the linear viscoelastic properties of entangled telechelic bulk metallo-supramolecular polymers. The latter are based on linear and star poly(*n*-butyl acrylate)s functionalized with a terpyridine ligand at each chain extremity, in the presence of transition metal ion of varying nature. The systems are investigated both experimentally and theoretically using small amplitude oscillatory shear and a modified version of the tube-based time marching algorithm (TMA), respectively. The experimental data reveal that sample relaxation depends on both disentanglement and association dynamics, with the respective importance of these two processes depending on the nature of the metal ion and on the temperature. A good description of the data is achieved using the modified TMA model, provided that dissociation events of metal-ligand complexes occur via ligand exchange. The model contains two fitting parameters, i.e., the fraction of unassociated stickers and the longest time needed in order to ensure that all the chains were dissociated at least once. This latter time is found to be independent of the chain architecture and is well described by an Arrhenius equation, which allows the derivation of the related activation energy. This work provides the necessary framework to explore other metallo-supramolecular networks, built from different chain architectures, and exploit the large richness of their dynamics. © *2017 The Society of Rheology*. [http://dx.doi.org/10.1122/1.4997593]

I. INTRODUCTION

Supramolecular polymers based on reversible physical associations form an interesting class of materials because of the richness in their tailorable properties compared to their nonassociating counterparts. Noncovalent bonds such as π–π stacking [1], hydrogen bonding [2], ionic interactions [3,4], or metal-ligand complexes [5] are sensitive to stimuli such as *p*H, irradiation, temperature, or mechanical forces, and their reversibility provides unique features such as healing [6,7], mechanosensitive and shape-memory properties [8,9]. Supramolecular polymers have potential applications in various domains, where a precise control over the molecular structure and properties is necessary such as drug delivery [10], tissue engineering [11], coatings [12], adhesives [13], and shock absorbers [14]. Regardless of the final application, the possible industrial exploitation of the transient nature hinges on the rheological behavior and resulting processability. In this respect, the design of smart materials of supramolecular polymers is dependent on our fundamental understanding of their structure and dynamics in the melt state. The latter are not only determined by the association/dissociation events of the transient interactions, but they are also governed by the internal dynamics of the building blocks (entanglements). Therefore, the influence of these two processes on the rheological properties and how they interact need to be addressed and understood.

Theoretical models on associating polymers have been mostly focused on static properties, in particular, the sol-gel transition, the aggregation of associating groups or the flower-like micelles bridged by flexible polymer chains [15–18]. Semenov and Rubinstein have developed a sticky Rouse model for unentangled polymers with many pairwise associating units per chain and considering that a sticker goes through many association and dissociation events with its old partner before finding a new sticker partner to associate with [19]. The sticky reptation model has been established to extend this idea to entangled associating polymers with many regularly spaced stickers in which polymer chains go through sticky Rouse motion along the confined tube to relax the stress [20]. Bedrov *et al.* performed standard molecular dynamic simulations of unentangled telechelic polymer solutions where associating groups are able to aggregate and form interlinked micellar clusters [21]. The stress relief in these systems was described as a two-step mechanism. First, a decay due to the translational motion or positional rearrangement of the end-groups inside their aggregates, and second by the fast hopping diffusion of end-groups between one micellar cluster into another one, which is then followed by the terminal relaxation due to cluster disintegration. Wang and coworkers studied the dynamics and rheology of unentangled telechelic polymer networks in which stickers with finite functionality are able to form interconnected clusters [22]. Their predictions revealed that the stress relaxation of such systems is governed by the partner exchange process rather than the single sticker hopping mechanism. The

[a]Author to whom correspondence should be addressed; electronic mail: flanco.zhuge@uclouvain.be
[b]Electronic mail: charles-andre.fustin@uclouvain.be
[c]Electronic mail: jean-francois.gohy@uclouvain.be
[d]Electronic mail: evelyne.vanruymbeke@uclouvain.be

partner (ligand) exchange process offers the stickers the possibility to bind to another partner in a new cluster without breaking all the sticky bonds formed in the initial cluster.

In the aforementioned studies, the simulations are essentially focused on unentangled associating systems or supramolecular polymers in solution. Furthermore, the polymeric spacers in between the stickers are relatively short, and the content of stickers is relatively high. Hence, in this type of systems, the attention focuses on the aggregate/cluster formation. On the contrary, when the spacers between stickers are long enough, the amount of incorporated associating moieties becomes minor compared to the polymer matrix, and the sticker density becomes negligible compared to the density of entanglements. As a result, the aggregation and/or cluster formation is less pronounced, and the associated domains can be seen as physical cross-linking points for the entangled chains. Theoretical models to explain the rheological properties and dynamics of such entangled telechelic systems are scarce [23,24]. One of the objectives of this work is to provide such a theoretical contribution, based on model polymers. In particular, this requires using telechelic chains characterized by pairwise supramolecular interactions, in order to avoid the formation of large, ill-defined aggregates. It also requires selecting a polymer, which can be studied under a large range of temperatures in order to have access to its full dynamics and to have many possibilities to vary the association strength of the reversible bonds.

Here, we investigate the linear viscoelastic properties of entangled telechelic polymers based on linear and star poly(*n*-butyl acrylate) P*n*BA that we synthesized and functionalized with a terpyridine (tpy) ligand (a pairwise sticker) at each chain extremity. Once transition metal ions are added, metal-ligand coordination occurs to form bis-tpy complexes, which play the role of transient junctions between the polymer chains [25]. Depending on the architecture of the polymer, rheological data show that the effect of stickers is the retardation of terminal relaxation by several orders of magnitude. Since the reference samples have a large molar mass and only contain the ligands at their extremities, the weight proportion of tpy in the samples is very low, ranging from 0.003 to 0.008 wt. %. Therefore, for all samples, the level of the plateau modulus stays governed by the entanglements density. Another consequence of this low density of ligands is the fact that we do not expect the formation of aggregates or large clusters of tpy due to phase separation, as it was observed for example in [26]. The absence of aggregate was further confirmed by wide angle X-ray scattering (WAXS) measurement (results not shown).

A refined version of the time marching algorithm (TMA) is developed to describe the experimental rheological properties. Model predictions are compared to systematic experimental data obtained from small angle oscillatory shear (SAOS) measurements, and the results are presented herein. The rest of this paper is organized as follows. In Sec. II, we summarize the experimental procedures to synthesize and characterize the associating polymeric models. Section III A presents the assumptions made and the additional parameters applied to TMA. The refined TMA for entangled sticky polymers is described in Sec. III B. Model predictions on the dynamic and rheological properties of entangled telechelic polymers are presented and discussed in Sec. IV. The conclusions are drawn in Sec. V.

II. MATERIALS AND EXPERIMENTAL

A. Materials

The synthesis of the linear ($M_n = 101$ and 142 kg/mol) and four-arm star ($M_n = 160$ and 249 kg/mol) P*n*BAs end-functionalized with tpy ligand (P*n*BA-tpy$_x$) was achieved by reversible addition-fragmentation chain-transfer (RAFT) polymerization in bulk condition [25]. Details on the precursor samples are given in Table I.

B. Sample preparation

Samples were prepared by dissolving a given amount of P*n*BA-tpy$_x$ in acetone. The sealed reaction vessels were sonicated and occasionally shaken to form homogeneous, concentrated solutions with a concentration of 500 g l^{-1}. The metallo-polymers were then readily obtained by adding 0.5 stoichiometric equivalents of transition metal ions (with respect to the tpy content) dissolved in acetone or methanol. The reaction vessels were again sonicated and shaken to ensure total complexation of the metal. The solvent was evaporated under vacuum to obtain homogenous metallo-supramolecular bulk polymers (MSBPs). All samples were prepared in stoichiometric conditions to promote the formation of complexes made by one metal ion coordinated by two tpy ligands. tpy moieties and trithiocarbonate functions are thermodynamically stable (during and after measurement) within the temperature range of study that we conducted.

The glass transition temperatures of the reference samples and the supramolecular polymers were determined by differential scanning calorimetry. No specific change of T_g was observed with the sample architecture or with the addition of the metal ions. Values ranging from −53 to −51 °C were found.

C. Rheological characterization

Shear rheological experiments were performed in the linear regime on an ARES (TA Instruments) strain-controlled rheometer equipped with a heat exchanger. All experiments were carried out at given temperatures, using 8 mm plate-plate geometries. The gap was adjusted between 400 and 500 μm so that the geometry was completely filled. All samples were equilibrated in the rheometer at a temperature of 130 °C, and normal forces were checked to be relaxed prior any measurement. Measurements were repeated for a period varying from a week to months, showing no aging of the materials. Samples were measured at several temperatures, ranging from $T = -20$ to 80 °C. For the reference samples, master curves were built at a reference temperature of 25 °C, following a Williams-Landel-Ferry (WLF) equation with the constant $c_1 = 7.63$ and $c_2 = 103.8$ K [27]. The vertical shift was applied in order to compensate for the density effect. The vertical shift factors, $b(T)$, can be expressed as $b(T) = [\rho(T_{ref}).T_{ref})/(\rho(T)\cdot T]$, where $\rho(T)$ is the density (g/cm^3) of the material at

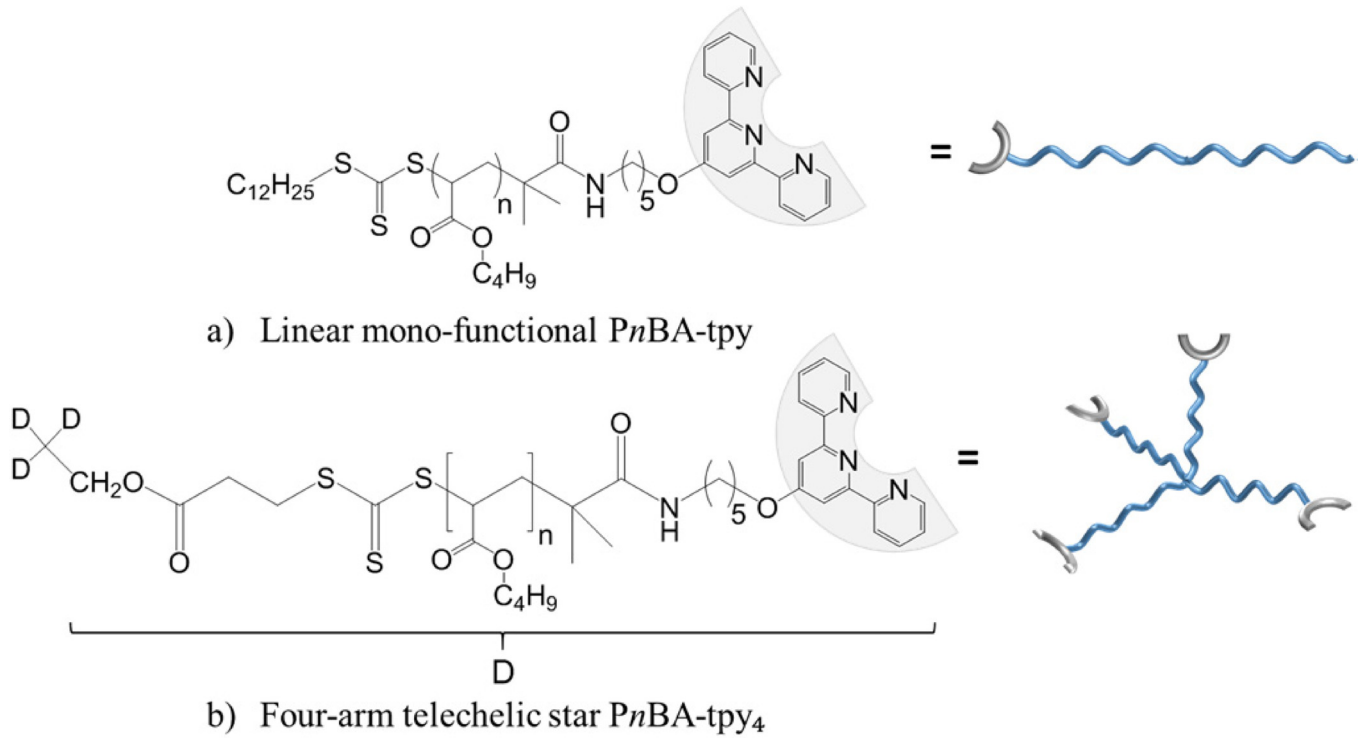

temperature T (K), and the reference temperature $T_{ref.} = 298$ K. In the case of P*n*BA, the temperature dependence of the density is given by $\rho(T) = 1.2571 - 6.89 \times 10^{-4}$ T [28,29]. Then, same shift factors were used to shift the viscoelastic data of the supramolecular polymers. In such a way, only the influence of temperature on the segmental dynamics is taken into account, which allows us to isolate its influence on the dynamics of the supramolecular bonds. Since the association dynamics of the stickers also depends on T, it is expected that the supramolecular polymers will exhibit complex rheological behavior.

III. MODELING THE VISCOELASTIC PROPERTIES OF SLIGHTLY ENTANGLED STICKY MOLECULES

A. Experimental observations and assumptions behind the model

In this section, the basic assumptions behind the modified TMA model, which is developed in Sec. III B, are detailed. As explained below, these assumptions are supported by experimental observations.

Since a good understanding of the molecular dynamics of the precursor samples is helpful in building a molecular picture for the supramolecular systems, we will first discuss the modeling of the rheological observations of the parent materials, which has been achieved by the use of the original TMA [23,30]. The latter is a tube based model that incorporates all the reorientation processes in the linear flow regime, namely reptation, contour length fluctuations (CLF), and constraint release (CR). It requires the use of three molecular parameters, which are topology independent, namely the entanglement plateau modulus G_N^0, the entanglement relaxation time τ_e, and the molecular weight between the entanglements M_e. The model predictions presented in Fig. 1 have been obtained using the following values: $G_N^0 = 160$ kPa, $\tau_e = 2.3 \times 10^{-4}$ s, $M_e = 18$ kg/mol, consistently with previous work [31]. Moreover, the number average molecular weights and dispersity have been optimized as followed: $M_n = 38.5$ kg/mol per arm and $Đ = 1.04$ for the Star160 k, $M_n = 66$ kg/mol per arm and $Đ = 1.08$ for the Star250 k, $M_n = 101$ kg/mol and $Đ = 1.08$ for the Lin100 k, and $M_n = 138$ kg/mol and $Đ = 1.08$ for the Lin140 k. These molar masses are within the 8% of variation with the experimental

TABLE I. Structural parameters of P*n*BA polymers functionalized with tpy ligand at chain extremity.

Samples	Description	$M_{n,\ system}$ [a]	$M_{n,\ arm}$ [a]	M_n/M_e [b]	Đ [c]
Lin100 k	Linear monofunctional PnBA-tpy	101 kg/mol	—	5.6	1.14
Lin140 k	Linear monofunctional PnBA-tpy	142 kg/mol	—	7.8	1.14
Star160 k	Four-arm telechelic star PnBA-tpy$_4$	160 kg/mol	40 kg/mol	2.2 per arm	1.25
Star250 k	Four-arm telechelic star PnBA-tpy$_4$	249 kg/mol	62 kg/mol	3.4 per arm	1.20

[a]Molar mass of whole system determined by ^{1}H-NMR.
[b]Number of entanglements calculated using $M_e = 18$ kg/mol.
[c]Molar mass dispersity of the polymers determined by SEC, polystyrene standards were used for calibration.

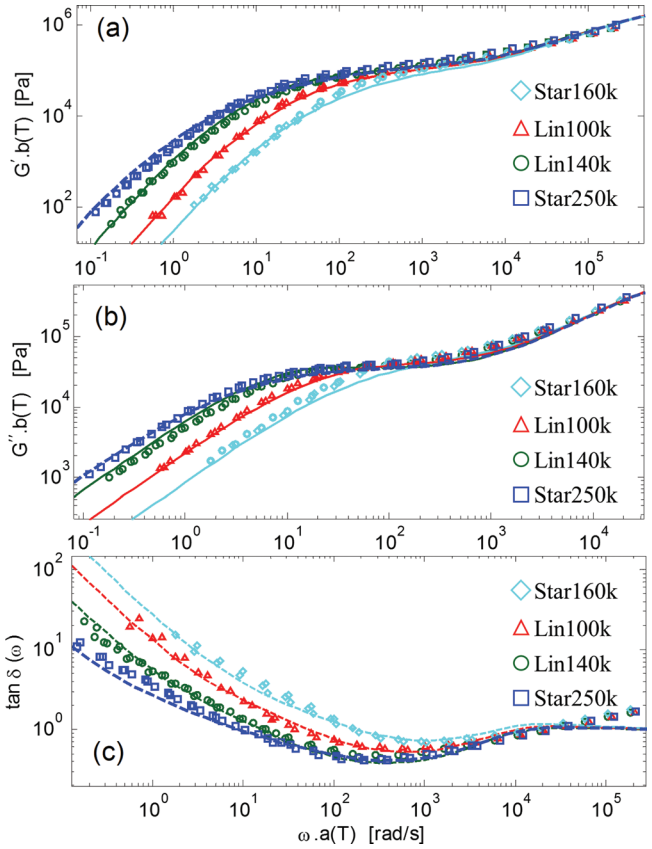

FIG. 1. Storage modulus (a), loss modulus (b) and tan δ curves of the reference star and linear polymers (cyan ◇: Star160 k, red △: Lin100 k, green ○: Lin140 k, and blue □: Star250 k). Symbols are experimental data and lines are model predictions. Master curves have been built at 25 °C.

values, while the optimized $Đ$ are systematically slightly smaller than the experimental values.

Figure 1 compares the theoretical (lines) and the experimental (symbols) response and phase angle of the reference telechelic star and monofunctional linear polymers. It demonstrates that chains are slightly entangled since all samples exhibit a short plateau region and have relatively short terminal relaxation times. At the reference temperature $T = 25$ °C, the values of the terminal times, τ_{rel}, are $\simeq$0.01 s for samples Star160 k and Lin100 k, and $\simeq$0.1 s for samples Star250 k and Lin140 k. Moreover, the comparison reveals that linear chains are short enough to relax their orientation, mainly by means of CLF as the star chains do. For example, the Lin140 k sample, which contains around 7.8 entanglements, has very similar τ_{rel} to the Star250 k sample. The fact that both linear and star chains are slightly entangled will be taken into account in assumption A2.

The black symbols in Fig. 2 show the viscoelastic response of the Star160 k+Cu supramolecular sample with a stoichiometric amount (0.5 eq.) of Cu ions as well as with an excess of ions (1 eq.). Despite the fact that the sample comprises metal-ligand interactions the value of the (apparent) plateau modulus stays close to the value of the entanglement plateau, i.e., 160 kPa, of the precursor P*n*BA chain [31]. This observation is typical for melts of associating chains in which the number of active functional groups per chain is lower than the number of entanglements per chain [32,33].

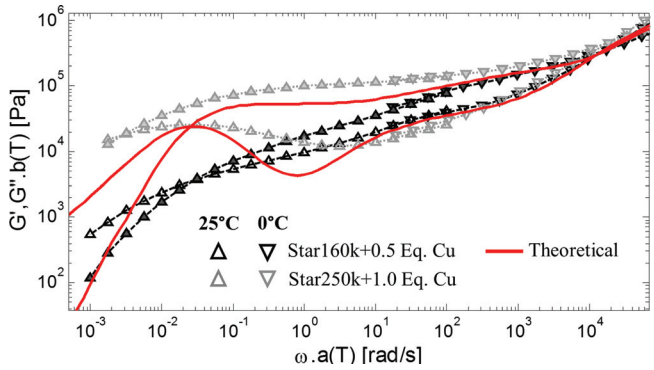

FIG. 2. Experimental storage (filled symbols) and loss (open symbols) moduli of Star160 k+Cu containing 0.5 eq. of Cu ions (black symbols), or 1 eq. of ions (gray symbols). The data have been measured at 25 °C (Δ) and 0 °C (δ) and shifted to the reference temperature of 25 °C. The continuous red curves in panel are the theoretical viscoelastic response of sample Star160 k with 0.5 eq. of Cu ions, assuming that 45 wt. % of arms are unassociated and considering an association time, τ_{ass}, equal to 60 s.

Hence, rather than reinforcing the plateau modulus, the main effect of the stickers (while active/associated) is to delay chain disentanglement, i.e., the terminal relaxation.

From the same curves of sample Star160 k containing 0.5 eq. of Cu ions, it is evident that at an intermediate frequency, the storage modulus undergoes a gradual decrease. The corresponding frequency range is comparable to one of the relaxations of the reference polymer (see Fig. 1). This suggests that part of the ligands is initially dissociated, i.e., they do not form transient interactions with metal ions, and have time to relax. Thus, despite the fact that the metal ions have been added in a stoichiometric amount in order to fulfil all the complexes, a large fraction of star arms are free and do not participate in the supramolecular network. This difficulty to create metal-ligand complexes is attributed to the low density of metal ions present in the sample, which reduces the probability of a chain end to meet a free ion and another free end in its surrounding. In order to reduce the amount of free dangling arms, the Cu ions must be added in excess, as it is illustrated by the gray curves, which were obtained by adding 1 eq. of Cu ions. In this last case, a longer and higher plateau is observed in the storage modulus curve. Thus, since a stoichiometric amount of metal ions has been added to the different supramolecular samples studied in this work (see Table II), we expect the proportion of dangling arms to be larger than the proportion obtained if we only account for their association/dissociation probability and equilibrium state.

Figure 2 also reveals the presence of polymer fractions (arms) having relaxation times much longer than the reference sample. This is because disentanglement of such fractions is prevented as long as their extremities are involved in metal-ligand complexes. Consideration of the two aforementioned experimental facts allows us to make the following assumption:

Assumption A1: Initially, i.e., at time $t = 0$, there are two different populations of ligands: the associated ones and the dissociated (or free) ones. Hereafter, these two populations will be referred to as population A and population F,

TABLE II. List of sample annotations and their descriptions.

Annotation	Description
Lin100 k+Zn	Linear monofunctional $PnBA_{788}$-tpy + 0.5 eq. $ZnCl_2$
Lin100 k+Cu	Linear monofunctional $PnBA_{788}$-tpy + 0.5 eq. $CuCl_2$
Lin100 k+Co	Linear monofunctional $PnBA_{788}$-tpy + 0.5 eq. $CoCl_2$
Lin140 k+Zn	Linear monofunctional $PnBA_{1108}$-tpy + 0.5 eq. $ZnCl_2$
Lin140 k+Cu	Linear monofunctional $PnBA_{1108}$-tpy + 0.5 eq. $CuCl_2$
Lin140 k+Co	Linear monofunctional $PnBA_{1108}$-tpy + 0.5 eq. $CoCl_2$
Star160 k+Zn	Four-arm telechelic star $PnBA_{1248}$-tpy_4 + 0.5 eq. $ZnCl_2$
Star160 k+Cu	Four-arm telechelic star $PnBA_{1248}$-tpy_4 + 0.5 eq. $CuCl_2$
Star160 k+Co	Four-arm telechelic star $PnBA_{1248}$-tpy_4 + 0.5 eq. $CoCl_2$
Star250 k+Zn	Four-arm telechelic star $PnBA_{1943}$-tpy_4 + 0.5 eq. $ZnCl_2$
Star250 k+Cu	Four-arm telechelic star $PnBA_{1943}$-tpy_4 + 0.5 eq. $CuCl_2$
Star250 k+Co	Four-arm telechelic star $PnBA_{1943}$-tpy_4 + 0.5 eq. $CoCl_2$

respectively. For a schematic representation of the system at $t = 0$ see Fig. 3. The same applies to the system made of monofunctional linear chains. Roughly speaking, the weight fractions of the two populations are similar.

As explained above (c.f. discussion of Fig. 1) the star arms are slightly entangled, and therefore, they renew orientation relatively fast. By utilizing this fact, we can safely consider the following:

Assumption A2: The star arms that belong to population F will fully relax by CLF before they associate. In other words, we assume that the fluctuation time for a full retraction is shorter than the average time a sticker spends in the dissociated state. Similarly, it is considered that a star arm which is initially associated and which dissociates at any time t will have enough time to fully disentangle before its sticker associates again.

The solid lines in Fig. 2 correspond to the model prediction found when (1) the weight fraction of free arms at time $t = 0$, i.e., of population F, is 45 wt. %, and (2) all stickers of population A have a single association lifetime τ_{ass}. The latter is defined by the inverse of the G′/G″ crossover frequency, and therefore, it is much longer than the terminal relaxation time of the precursor material. To avoid possible confusion, we stress that the model predictions here do not correspond to the original version of the TMA for nonassociating chains, but to a special case of the modified TMA for associating chains, which is presented below. Comparison of the model predictions and the data demonstrates two points. First, in the frequency range 10^4–10^1 rad/s, the slow decrease of the moduli is well captured by the fast relaxation of the free arms that bear a ligand of population F. In other words, the arms that are ended by a free ligand. Second, the terminal response cannot be reproduced by assuming a unique association lifetime τ_{ass} for all the ligands of population A. Such an assumption results in a Maxwell-like terminal relaxation characterized by a single exponential decrease of the form $\exp(-t/\tau_{ass})$, which is clearly not the case for the experimental data, which show large relaxation time spectrum. This result was not expected since all the metal-ligand complexes are of same nature, and therefore, should have a similar bonding energy and association time. In order to explain this departure from a Maxwell-like behavior, we consider that a chain end never dissociates by itself, but rather dissociate thanks to a process of ligand exchange around the ions. It is similar to the mechanism suggested by Wang and coworkers to describe the dynamics in supramolecular polymer networks formed by associating telechelic chains [22]. There, it was demonstrated that in the case of unentangled telechelic polymers, the energy related to sticker (ligand) exchanges is much lower than the energy cost to dissociate a sticker from an ion through hopping process, without replacing it with another one. Thus, the necessary time for a sticker to dissociate by ligand exchange is expected to be much shorter than the dissociation time of a sticker unable to beneficiate from the presence of free dangling arms in its surrounding. This is in agreement with the results of Fig. 2, where it is observed that the star arms are relaxing much slower when the proportion of dangling arms is reduced. Therefore, we adopt the ligand exchange mechanism in our systems containing a stoichiometric amount of metal ions. This leads to the following assumption regarding our modified TMA model:

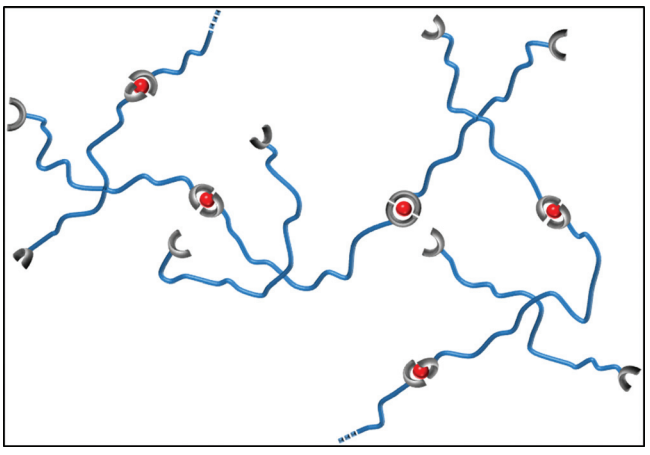

FIG. 3. Schematic representation of telechelic star polymers in the presence of two different ligand (sticker) populations.

Assumption A3: The association/dissociation events are achieved via ligand exchanges between free and associated populations [see panels (a) and (b) of Fig. 4 for a schematic representation]. Nevertheless, we anticipate that most of the ligand exchanges are inefficient in allowing new arms to relax. In other words, it is likely that the ligand exchange occurs among arms that have been already relaxed, and therefore, such event cannot further contribute to the polymer relaxation. For example, consider the case illustrated in panel (c) of Fig. 4 (red dotted circle): here, the ligand exchange takes place between a ligand of population F and a ligand that initially belonged to population A but had the possibility to fully relax in a previous step [see panel (b)]. In this respect, it seems realistic to consider that the number of these inefficient exchanges increases with time since the fraction of relaxed material increases with time as well.

Moreover, some stickers could be trapped around a specific metal ion, meaning that they dissociate and associate again with the same ion, canceling their dissociation step in this manner. Such stickers do not have the possibility to easily find another ligand in the surroundings. In either case, it

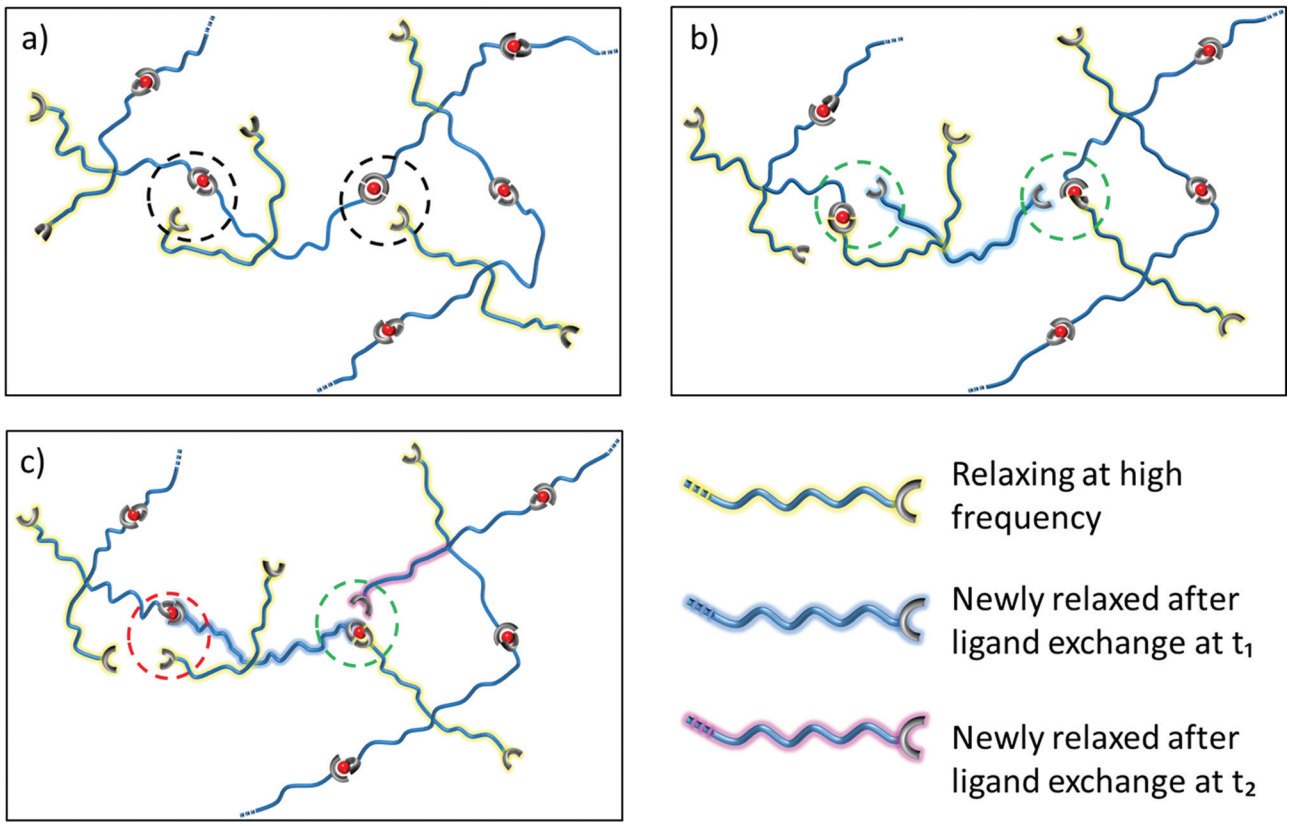

FIG. 4. Schematic representation of ligand exchange mechanism on telechelic star polymers (a) at $t = 0$, (b) at $t = t_1$, and (c) at $t = t_2 > t_1$.

is expected that the probability for new arms to relax is becoming extremely low through time. In consequence, the time needed for the stickers initially associated to dissociate for the first time exhibits very broad polydispersity, which explains the strong deviation from a Maxwell-like terminal relaxation behavior. In the model, to quantify this polydispersity, we will make the following assumption:

Assumption A4: Since a ligand exchange taking place when a fraction $1/n$ of the arms are unrelaxed it is approximately n times less efficient than an initial exchange; herein, we assume that the times needed for the associated stickers to dissociate for the first time (and thus, to start contributing to the polymer relaxation) are equally distributed on a log time scale. It should be stressed that this time distribution does not represent the distribution of times after which a sticker will dissociate, but it rather represents the distribution of times after which a sticker attached to an unrelaxed arm will dissociate. Somehow, it represents the distribution of the *effective* association times. As shown in Fig. 5, we consider these times to be distributed between $\tau_{exchange}$ and τ_{final}. The first time represents the minimum waiting time needed to observe the dissociation of some arms. It can be seen as the "internal clock" of the supramolecular bond dynamics, which dictates the rhythm at which the ligand exchanges are observed. The second time τ_{final}, corresponds to the longest effective association time of the stickers. Notice that $\tau_{exchange}$ must be rather small since before this time none of the associated ligands can dissociate. Therefore, a large value would lead to the appearance of a second plateau in the storage modulus at an intermediate frequency as observed in Fig. 2, with single, long association time. Herein, we consider a constant value for $\tau_{exchange}$, which governs the onset of the ligand exchange process. (See discussion below for explanation of this choice). Thus, the parameter τ_{final} is the only parameter, which must be defined in order to determine the distribution of effective association times of the stickers. While considered as a fit parameter in the model, it will be shown in Sec. IV that this relaxation time has a physical meaning and follows an exponential dependence on activation energy.

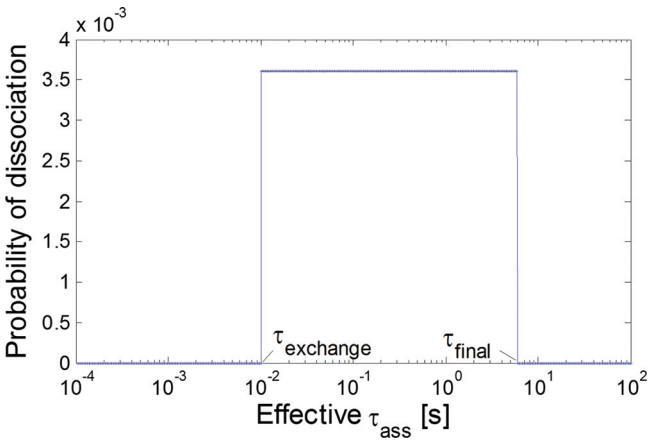

FIG. 5. Example of distribution of *effective* association times taken in the model, assuming that $\tau_{exchange} = 0.01$ s and $\tau_{final} = 6$ s. This distribution represents the probability for an associated sticker to detach for the first time at the corresponding effective association time.

This way of determining the *effective* association time distribution allows us to simply account for the fact that the majority of the arms are dissociating at short times (i.e., after few $\tau_{exchange}$), while allowing some of them to have very long association times.

The influence of $\tau_{exchange}$ and τ_{final} is shown in Fig. 6. In this example, we consider that the proportion of associated arms $p_{ass,}$ is equal to 60 wt. %. (A detailed discussion concerning p_{ass} follows further down in this section.) The predictions shown in Fig. 6 are based on the model described in Sec. III B.

While it is clear that the predictions are strongly sensitive to the value of τ_{final}, the results obtained for different values of $\tau_{exchange}$ are similar when this parameter is becoming short. Generally, one can estimate $\tau_{exchange}$ by looking at the experimental data, in particular at the frequency at which the storage modulus starts to decrease faster than expected if we consider that the star arms cannot exchange their ligands. It was found that it should be around 0.01 s. Based on Fig. 6(b), we do not expect a large influence of this parameter; therefore, we consider it as a constant, i.e., $\tau_{exchange} = 0.01$ s for all the samples at $T = 25\,^{\circ}$C. In a way, this time can be seen as the "clock" of the supramolecular dynamics, i.e., which fixes the rhythm at which we are observing the ligand exchanges, while the ratio $(1/\tau_{final})$ is related to the number of exchanges observed at each time step.

Thus, the model contains only two unknown parameters: the longest association time of the stickers τ_{final}, and the proportion of associated arms p_{ass}. It must be noted that the longest association time τ_{final}, cannot be determined from the G′-G″ crossover at low frequency. Indeed, as discussed in Sec. IV, the terminal relaxation time of these samples includes both dissociation dynamics and disentanglement dynamics. Therefore, its value is expected to be larger than τ_{final}.

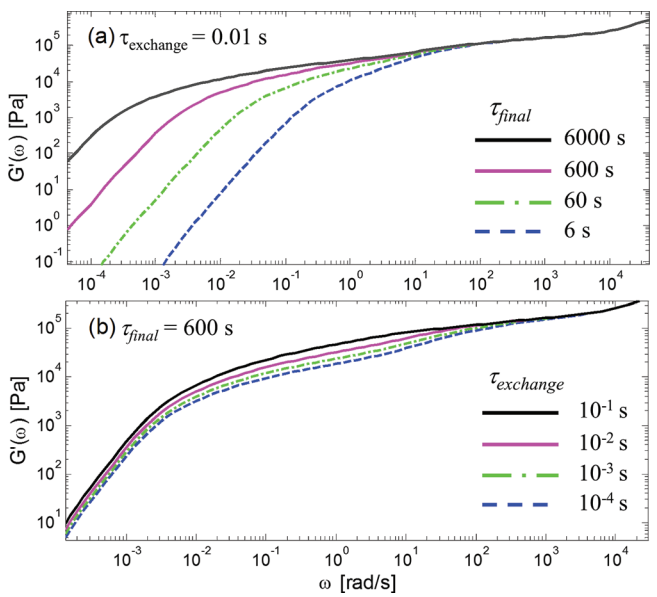

FIG. 6. Influence of $\tau_{exchange}$ and τ_{final}. (a) The value of $\tau_{exchange}$ is fixed to 0.01 s and the value of τ_{final} is equal to 6 s (--), 60 s (-·), 600 s (—), or 6000 s (—); (b) the value of τ_{final} is fixed to 600 s and the value of $\tau_{exchange}$ is equal to 10^{-4} s (--), 10^{-3} s (-·), 10^{-2} s (—) or 10^{-1} s (—).

We now turn our attention to the latter parameter, i.e., p_{ass}, for which we make the following assumption:

Assumption A5: The average fraction of associated arms p_{ass}, is constant through time (the arms of population A initially). This means that each time an arm becomes free, another one becomes associated, in agreement with the idea of ligand exchanges. However, note that the arm that becomes associated might have already relaxed through a previous ligand exchange event.

The parameter p_{ass} is fixed from the experimental data, by determining the proportion of arms, which are able to relax at short times, i.e., at high frequency. Since the predictions are quite sensitive to this parameter, its value can be fixed with an accuracy of around 5%. Usually, values around 50 wt. % are found, which are quite low. This means that the average time during which a freshly/newly dissociated sticker will stay free is quite long. This also means that at each time step ($\tau_{exchange}$), only a few of the free stickers are able to create an exchange of ligands. As already mentioned, this can be understood by considering the low density of stickers and the slow diffusion process of the chains, leading to the presence of dangling arms, which do not find a metal-ligand complex in their surroundings. The presence of a small fraction of nonfunctionalized arms must also be envisaged. It must be noted that in the case of an entangled telechelic polymer, the fact that two arms of the same star can associate and create a polymer loop is not expected to enhance the proportion of fast relaxing polymers. Indeed, in order to disentangle, the polymer loops must also dissociate. The values of p_{ass} and τ_{final} are discussed in Sec. IV. In Sec. III B, we assume that they are known, and present the model that we developed in order to account for the sticker dynamics.

All assumptions described above are applied to linear monofunctional polymers as well. Nevertheless, in the case of the monofunctional chains, the terminal relaxation times are limited by the possible reptation of the whole self-assembly, which is composed of two linear chains associated through metallo-supramolecular bonds at the center as depicted in Fig. 7.

B. Modified TMA model

Based on the assumptions presented in Sec. III A, we can now extend our TMA model to the specific case of slightly entangled telechelic chains. A specificity of the systems studied in this work is the fact that the relaxation time of a free arm is shorter than the time during which a sticker stays free. Therefore, the model is based on the idea that once an arm is

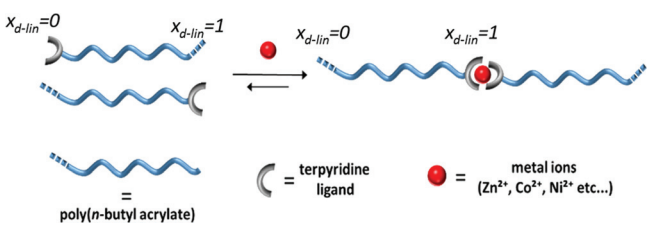

FIG. 7. Self-assembly of associating linear semitelechelic polymers.

dissociated, it has enough time to relax (see Assumptions A2 and A5). In case of very long, well entangled, polymers, this would not be the case anymore, and one should also consider the situation in which an arm is able to fully relax only after several dissociation/association blinking events.

1. TMA model

We first briefly describe the main equations behind the TMA model [34], as it is used for describing the viscoelastic properties of the reference samples and serves as the starting point of our modified model. A more detailed explanation can be found in [30,35]. It must be noted that in TMA the linear chains are considered as 2-arm stars, which are able to relax by reptation.

In this model, the relaxation modulus as a function of time $G(t)$, accounts for both the high frequency Rouse process $G_R(t)$, and the disentanglement modulus $G_d(t)$, [36]

$$G(t) = G_{\mathrm{R}}(t) + G_{\mathrm{d}}(t) \tag{1}$$

with

$$G_{\mathrm{R}}(t) = \sum_k \frac{\upsilon_k \rho RT}{M_{arm,k}} \left\{ \frac{1}{4} \sum_{p=1}^{Z_k} \exp\left(-\frac{p^2 t}{\tau_{\mathrm{R}}(M_{arm,k})} \right) + \sum_{p=Z_k+1}^{n} \exp\left(-\frac{2p^2 t}{\tau_{\mathrm{R}}(M_{arm,k})} \right) \right\}. \tag{2}$$

In Eq. (2), υ_k and $\tau_R(M_{arm,k})$ represent the weight fraction and the Rouse time of an arm of chain k, respectively. Z_k represents the number of entanglements in an arm of chain k; the parameter ρ is the monomeric density, R is the gas constant and T is the temperature.

The disentanglement modulus and the plateau modulus G_{N}^0 are defined as

$$G_{\mathrm{d}}(t) = G_{\mathrm{N}}^0 \varphi'(t) \{\phi(t)\}^{\alpha}, \tag{3}$$

$$G_{\mathrm{N}}^0 = \frac{4}{5} \frac{\rho RT}{M_e} \tag{4}$$

with $\varphi'(t)$ being the unrelaxed fraction of initial tube segments and α the dynamic dilution exponent, which is fixed here to 1 [37]. CR mechanisms are taken into account by the dilation factor $\phi(t)$, which defines the diameter a of the dilated tube [$a = a_0 \cdot \phi(t)^{-\alpha/2}$, with a_0 as the initial tube diameter]. As long as the polymer relaxation occurs gradually, the dilation factor $\phi(t)$ is equal to the unrelaxed fraction of initial tube segments $\varphi'(t)$ [35]. This last parameter can be determined by looking at all molecular segments $x_{arm,k}$, from $x_{arm,k} = 0$ at the extremity of an arm to $x_{arm,k} = 1$ at the middle of all arms (in proportion υ_k), and by determining if they are still moving in their initial tube or not, i.e., if they are not yet relaxed through reptation or CLFs mechanisms

$$\varphi'(t) = \sum_k \upsilon_k \int_0^1 p_{fluc}(x_{arm,k}t) p_{rept}(x_{arm,k}t)\, dx_{arm,k}. \tag{5}$$

In this equation, the survival probability related to the reptation process $p_{rept}(x_{arm,k},t)$ is either fixed to 1 in case of a star molecule (since it cannot reptate), either determined, based on the Doi and Edwards equation in case of a linear chain [38]

$$p_{rept}(x_{arm,k}, t) = \sum_{podd} \frac{4}{p\pi} \sin\left(\frac{p\pi x_{arm,k}}{2} \right) \exp\left(\frac{-p^2 t}{\tau_{rept}(2M_{arm,k})} \right). \tag{6}$$

In such a case, since linear chains of molar mass M_k are described as 2-arm stars which are able to reptate, they contain two arms of molar mass $M_{arm,k} = M_k/2$, and their corresponding reptation time is described as

$$\tau_{rept}(M_k = 2\,M_{arm,k}) = 3\,\tau_e \left(\frac{2\,M_{arm,k}}{M_e} \right)^3. \tag{7}$$

On the other hand, the survival probability related to the fluctuations process $p_{fluc}(x_{arm,k},t)$ is considered as equal to $\exp[-t/\tau_{fluc}(x_{arm,k})]$, in which the fluctuation time is determined by taking into account both the early fluctuations of the chain ends, and the deeper, activated, retraction of the arms

$$\tau_{early,arm}(x_{arm,k}) = \frac{9\pi^3}{16} \tau_e \left(\frac{M_{arm}}{M_e} \right)^4 {x_{arm,k}}^4, \tag{8a}$$

$$\tau_{activated}(x_{arm,k}) = \ln \tau_{activated}(x_{arm,k} - \delta x_{arm}) + 3 \left(\frac{M_{arm}}{M_e} \right) x_{arm,k}\, \phi(x_{arm,k})^{\alpha} . (\delta x_{arm}), \tag{8b}$$

$$\tau_{fluc,arm}(x_i) = \tau_{early,arm}(x_{tr}) \exp\left(\frac{\tau_{activated,arm}(x_i)}{\tau_{activated,arm}(x_{tr})} \right). \tag{8c}$$

In Eq. (8b), it is considered that the molecular segment located just before the segment $x_{arm,k}$ is positioned at $(x_{arm,k} - \delta x_{arm})$. The function $\phi(x_{arm,k})$ represents the polymer fraction which is not yet relaxed at the time the segment $x_{arm,k}$ of the arm is relaxing [39]. (In the case of the monodisperse sample, we would have $\phi(x_{arm,k}) = \phi(x_{arm}) = [1 - x_{arm}]$.) In Eq. (8c), the position x_{tr} represents the position of the arm segment at which the potential is equal to kT, i.e., at which the transition between early fluctuations and deep retraction is taking place.

2. Telechelic star molecules

In order to predict the linear viscoelastic properties of the telechelic star molecules, we start from the fact, that at time $t = 0$ there are two different populations of arms: A fraction p_{ass} of arms which are associated (and belong to population A), and a fraction $(1 - p_{ass})$ of dissociated arms (which belong to population F). Following assumptions A1 and A2, the free arms will be able to relax before becoming associated. Their fluctuation times are determined, based on Eq. (8).

It must be noted that in this case, the parameter $\phi(x_{arm,k})$ in Eq. (8b) must be determined by accounting for the fact that part of the arms cannot relax (thus, in case of monodisperse stars, we would have $\phi(x_{arm,k}) = \phi(x_{arm}) = [p_{ass} + (1 - p_{ass}).(1 - x_{arm})]$).

On the other hand, the associated arms have first to dissociate, before being able to fluctuate and relax. Since the storage modulus is mainly dominated by the entanglements and since the arms forming intra-associations are also entangled, it is expected that these last arms contribute to the sample relaxation in a similar way as the interconnected arms. As described in Sec. III A, a distribution of effective associate times ($\tau_{eff,ass,j}$, $\upsilon_{eff,ass,j}$) must be considered in order to account for the time decreasing probability to detach an unrelaxed arm through the exchange of ligand, and thus, to correctly describe the relaxation of these telechelic systems. Therefore, the survival probability of a specific segment $x_{arm,k}$ of an arm of mass M_k is described as:

$$p_{fluc}(x_{arm,k}, t) = \sum_j \upsilon_{eff,ass,j} \exp\left(\frac{-\max\left(0, (t - \tau_{eff,ass,j})\right)}{\tau_{fluc}(x_{arm,k})}\right). \tag{9}$$

By adding the condition according to which $(t - \tau_{eff,ass,j})$ is always positive, this equation can also be used at a time shorter than the effective association time $\tau_{eff,ass,j}$. Indeed, in such a case, the survival probability of the associated arms is simply equal to 1. Then, by using Eq. (9) in Eq. (5), the unrelaxed fraction of initial tube segments at time t is determined, which allows us to calculate the relaxation modulus $G(t)$ based on Eq. (3).

3. Monofunctional linear chains

Monofunctional linear chains can only be associated at one extremity, on which a tpy ligand is attached. Therefore, chains can only relax either as simple (dissociated) chains or as double (associated) chains. Since the average times during which a chain stays associated or free are rather long, and since the reptation time of a double chains (i.e., a pair of associated single chains) is only around eight times slower than the single chains, it is expected that most of the molecules do not have time to change their association status before being fully relaxed [25]. However, there is a small fraction of the double chains, which will relax by dissociation followed by the reptation of the single chains, especially when a weaker metal ion is used. Therefore, it is important to account for the possibility of the chain extremity to dissociate.

To this end, the same approach as proposed for the star polymers is followed. However, there are specific points which must be included in the model. The first point is the fact that the length of the relaxing chain can vary, from single to double. Therefore, it is important to define a common coordinate system to localize a specific molecular segment. Here, as illustrated in the cartoon in Fig. 7, we take the double chain as reference chain, with ($x_{d\text{-}lin} = 0$) as one of its extremity and ($x_{d\text{-}lin} = 1$) for its middle segment. This means that in the case, the chains are dissociated and relaxed as single chains since one of the double chains stays as the reference system, one needs to consider that these double (unassociated) chains are able to relax from their middle in order to keep consistency between the two statuses. Indeed, if the double chain is dissociated, its middle segment becomes an extremity of the single chain, i.e., its relaxation time $\tau_{rel}(x_{d\text{-}lin} = 1)$ is shorter than the relaxation of the middle segment of the single chain, $\tau_{rel}(x_{d\text{-}lin} = 0.5)$. A second specificity of the monofunctional chains is the fact that they can always relax as double or single chains.

Therefore, if a chain k is associated at time $t = 0$, it belongs to the population A and the survival probability of one of its molecular segment $x_{d\text{-}lin,\ k}$ at time t can be described as:

$$p(x_{d-lin,k}, t, A) = \sum_j \upsilon_{eff,ass,j} . \exp\left(\frac{-\min(t, \tau_{eff,ass,j})}{\tau_{rel}(x_{d-lin,k}, 2M_w)}\right) \cdot \exp\left(\frac{-\max\left(0, (t - \tau_{eff,ass,j})\right)}{\tau_{rel}(x_{d-lin,k}, M_w)}\right). \tag{10}$$

In this equation, we use the relaxation times τ_{rel}, rather than the corresponding reptation and fluctuations times, in order to keep the model simple (thus, approximating the survival probability $p_{rept}(x,t)$ by a single exponential $\exp(-t/\tau_{rept})$, rather than using Eq. (6). Note that this approximation is negligible. As long as the double chain stays associated, the relaxation time $\tau_{rel}(x_{d\text{-}lin,k}, 2M_w)$ of its molecular segment $x_{d\text{-}lin,k}$, is then described as

$$\tau_{rel}(x_{d-lin,k}, 2M_w) = \left(\frac{1}{\tau_{rept}(x_{d-lin,k}, 2M_w)} + \frac{1}{\tau_{fluc}(x_{d-lin,k}, 2M_w)}\right)^{-1} \tag{11}$$

with the reptation time and fluctuation time determined as for a covalent double chain [see Eqs. (7) and (8)] relaxing in a blend composed by a fraction p_{ass} of double chains and $(1 - p_{ass})$ of single chains.

Same expressions can be used for the single chains relaxation, but this requires first determining the corresponding reptation and fluctuations time in the usual coordinate system of a single chain, i.e., from $(x_{s\text{-}lin} = 0)$ at the extremity of the single chain, to $(x_{s\text{-}lin} = 1)$ at the middle, and then by transposing the results in the reference coordinate systems, $x_{d\text{-}lin}$, based on the double chains

$$\tau_{rel}(x_{d-lin,k}, M_w) = \tau_{rel}(x_{s-lin,k} = 2\ min\{x_{d-lin,k},\ (1 - x_{d-lin,k})\}, M_w). \tag{12}$$

In order to illustrate Eq. (10), the evolution through time of the survival probability $p(x_{d-lin,k}, t, A)$ is shown in Fig. 8, for single chains of molar mass M_n of 101 kg/mol, i.e., with a relaxation time of 0.15 s, while the relaxation time of the double chain is equal to 1.22 s. In this example, the

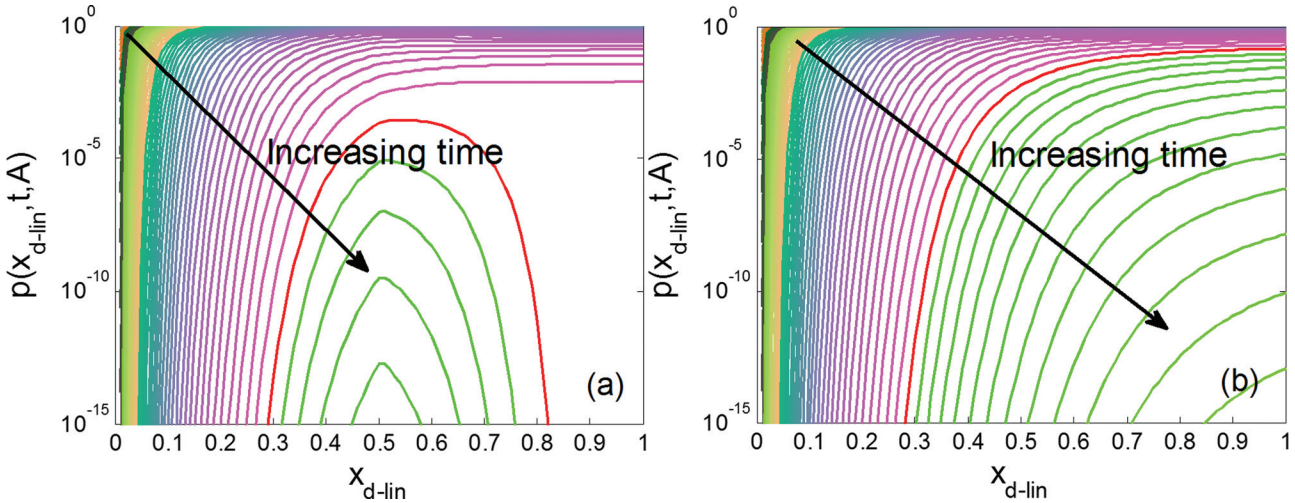

FIG. 8. Survival probabilities $p(x_{d-lin}, t, A)$ of the molecular segments of mono-functional monodisperse linear chains associated at time $t = 0$, from $x_{d\text{-}lin} = 0$ at the extremity of the double chain to $x_{d\text{-}lin} = 1$ at the middle. The corresponding single chains have a molar mass M_n of 101 kg/mol (i.e., a relaxation time of 0.15 s, while the relaxation time of the double chains is 1.22 s), and $p_{ass} = 0.5$. The distribution of effective association times is built by considering either $\tau_{final} = 1$ s (a), or $\tau_{final} = 100$ s (b).

distribution of effective association times has been built by considering either $\tau_{final} = 1$ s in Fig. 8(a) or $\tau_{final} = 100$ s in Fig. 8(b) (while $\tau_{exchange}$ has a fixed value, equal to 0.01 s). By considering $\tau_{final} = 1$ s, which is slightly shorter than the reptation time of the double chain, part of chain relaxes thanks to the dissociation of the ligand followed by the relaxation of the single chains [see Fig. 8(a)]. On the other hand, we observe that the chains characterized by a longer effective association time, $\tau_{final} = 100$ s, will basically relax as a binary blends composed of single and double chains [see Fig. 8(b)].

On the other hand, we assume that the chains which are not associated at time $t = 0$ (thus, which belong to the population F) have time to fully relax before their association. Therefore, their relaxation time can be determined as described in Eq. (12), following Assumptions A1 and A2:

$$p(x_{d-lin,k}, t, F) = \exp\left(\frac{-t}{\tau_{rel}(x_{d-lin,k}, M_w)}\right). \quad (13)$$

Finally, the survival fraction of initial tube segments at time t, $\varphi'(t)$, is determined, based on Eqs. (10) and (13)

$$\varphi'(t) = p_{ass} \sum_k \upsilon_k \int_0^1 p(x_{d-lin,k}, t, A) dx_{d-lin,k} + (1 - p_{ass}) \sum_k \upsilon_k \int_0^1 p(x_{d-lin,k}, t, F) dx_{d-lin,k}. \quad (14)$$

Together with Eqs. (1)–(4), we can determine the relaxation modulus $G(t)$ of these samples, and compare the theoretical results with the experimental data (see Sec. IV). As already mentioned, this model contains two unknown parameters, p_{ass} *and* τ_{final}. They will be first considered as fit parameters. Then, we will analyze their value in order to understand how they are varying.

IV. RESULTS AND DISCUSSION

Generally, the dynamics of these associating polymers are affected by both the disentanglement process of polymer chains and the dissociation process of the stickers. Depending on the architecture of the macromolecules, the temperature and the strength of metal-ligand complexes, one process is dominant compared to the other one. Below, we will examine each case systematically, starting from the influence of the temperature.

A. Influence of the temperature

Figure 9 presents the experimental data of the telechelic Star160 k+Cu and Star250 k+Cu samples at different temperatures.

As it is seen in Fig. 9(a), at high temperature ($T = 60\,^{\circ}$C), the stickers are weak and consequently the relaxation process is mainly governed by the disentanglement mechanism of CLFs, which are longer for the Star250 k+Cu material since it has arms longer than the other star polymer (see Table I).

At lower temperatures, however, the sticker lifetime becomes longer than the fluctuation time of the arms, and therefore, the process of sticker dissociation dominates the terminal relaxation of the star systems [c.f. Figs. 9(b) and 9(c)]. Thus, similar terminal times are observed for the two telechelic star samples, despite their difference in arm lengths. As will be seen below, the longest effective association time is identical for both star polymers. However, the influence of the arm length is noticeable at the intermediate frequency, where we observe that the star arms, which are not associated, are able to relax. This influence is highlighted in Fig. 9(d), which represents the $\tan\delta$ curves of these samples. This is consistent with Assumption 1, according to which part of the arms are free and can relax at short times.

Figures 10 and 11 compare the predictions of our modified TMA model (lines) with the experimental data (symbols), for these two star polymers, in the presence of a

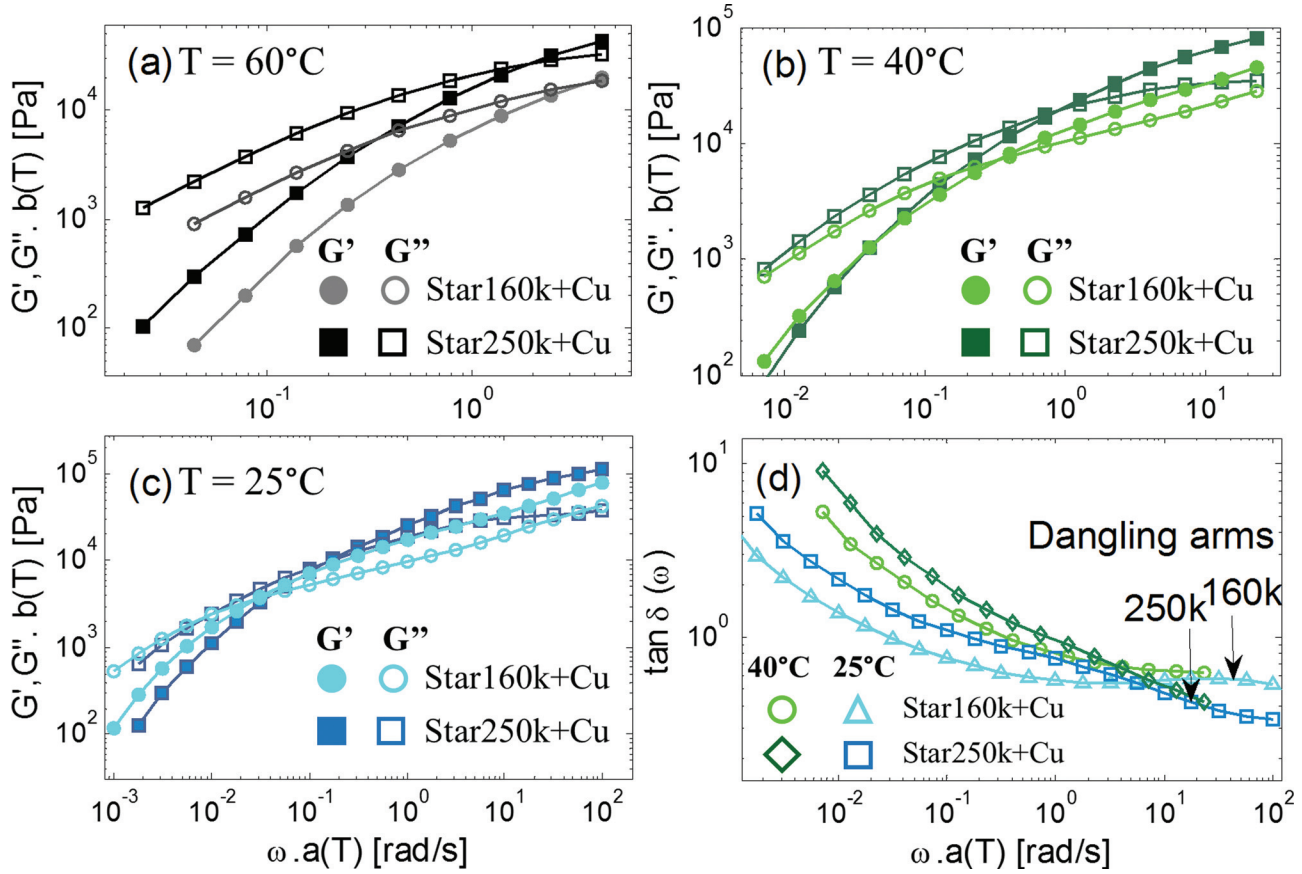

FIG. 9. Storage (filled symbols) and loss (open symbols) moduli of the telechelic Star160 k+Cu (○) and Star250 k+Cu (□), at (a) $T = 60\,^{\circ}$C, (b) $T = 40\,^{\circ}$C and (c) $T = 25\,^{\circ}$C; (d) tan δ curves of Star160 k+Cu at 40 °C (○) and 25 °C (△), and of Star250 k+Cu at 40 °C (◇) and 25 °C (□).The data have been shifted to a reference temperature of 25 °C, based on the shift factors determined for the reference samples.

stoichiometric amount of copper ions and at several temperatures. From those figures, it is evident that the model captures well the viscoelastic behavior of the samples. Concerning the two model parameters, namely the longest (effective) association time τ_{final}, and the fraction of associated arms p_{ass}, we find that identical values can be used for both systems, i.e., independently from the chain length. Furthermore, we notice that p_{ass} is temperature independent, whereas τ_{final} varies with temperature, from 5 s at high temperature ($T = 60\,^{\circ}$C) to 5000 s at low temperature ($T = 0\,^{\circ}$C). We anticipate these values to follow an exponential decrease with temperature (see the analysis of this parameter below). The fact that p_{ass} is temperature independent and τ_{final} is temperature dependent confirms our hypothesis that these two parameters are not directly related, as suggested in Sec. III A, due to the presence of dangling arms, which could not find any partner in their surroundings to associate. Also, if the fraction of associated stickers was only dependent on the association and dissociation kinetics of the stickers, we would expect p_{ass} to decrease with T, which is not observed here. This is again attributed to the dominant effect of the dangling arms unable to find a free ion, which does not seem to be affected by the temperature.

In Fig. 11, it is observed that at high temperature $T = 80\,^{\circ}$C, the sample mostly relaxes as the reference sample [see Fig. 1(a)], i.e., with a negligible effect on the supramolecular association. On the other hand, the influence of associated sticker is clear at low temperature.

B. Influence of the chain architecture

In this section, we discuss the influence of the chain topology on the viscoelastic response. For this reason, we compare the response of star and linear molecules associating via copper complexes. Figure 12 shows such a comparison for Lin100 k+Cu and Star160 k+Cu (see Table II). One will have to keep in mind that the arm molecular weight of the stars (40 kg/mol) is smaller than half the molecular weight of the linear chains, which leads to a faster relaxation of the reference star sample. However, the situation is inverted once the ions are added to the polymer. From Fig. 12 it is evident that the polymers based on the monofunctional linear chains relax much faster than the telechelic star molecules. This behavior suggests that, contrary to star polymers, there is an upper limit in the terminal relaxation time of the linear chains. In theory, this upper limit would correspond to the relaxation time of the double linear chain, i.e., two monofunctional chains linked together through transient bonds. In other words, even if some of the transient associations have an effective lifetime that is much longer than the terminal time of the precursor, the sticker effect will not translate to further retardation of the terminal relaxation since the supramolecular chains can reptate as doubled linear chains.

To examine this behavior further, we plot together in Fig. 13 the experimental data for samples Lin100 k+Cu and Lin140 k+Cu at several temperatures. We observe that data nearly overlap, despite the large difference observed in the

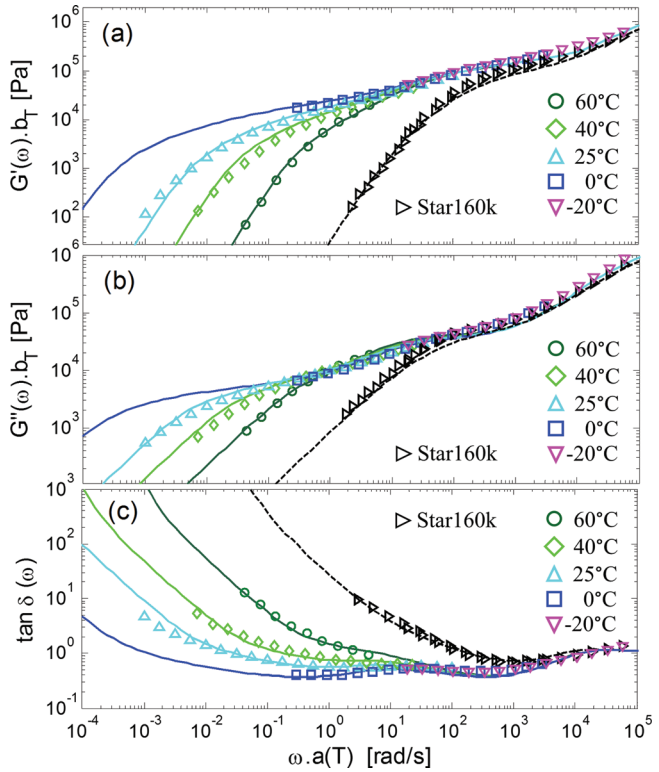

FIG. 10. (a) Storage modulus, (b) loss modulus, and (c) tan δ curves of the reference sample Star160 k (black, ▷) and of the telechelic Star160 k+Cu measured at temperature $T = 60\,^{\circ}$C (dark green, ○), 40 °C (green, ◇), 25 °C (cyan, △), 0 °C (blue, □), and −20 °C (magenta, δ). The experimental data (symbols) have been shifted to a reference temperature of 25 °C, based on the shift factors determined for the reference samples. The theoretical curves (continuous and dashed curves) have been obtained by fixing $p_{ass} = 0.45$ and $\tau_{final} = 5$ s at 60 °C, 50 s at 40 °C, 250 s at 25 °C, and 5000 s at 0 °C.

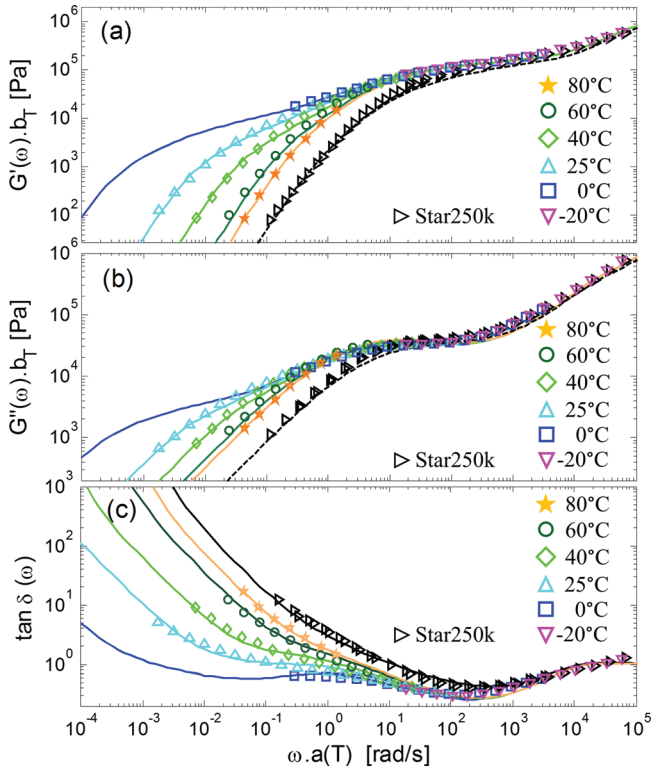

FIG. 11. (a) Storage modulus, (b) loss modulus, and (c) tan δ curves of the reference sample Star250 k (black, ▷) and of the telechelic Star250 k+Cu measured at temperature $T = 80\,^{\circ}$C (orange, ★), $T = 60\,^{\circ}$C (dark green, ○), 40 °C (green, ◇), 25 °C (cyan, △), 0 °C (blue, □), and −20 °C (magenta, δ). The experimental data (symbols) have been shifted to a reference temperature of 25 °C, based on the shift factors determined for the reference samples. The theoretical curves (continuous and dashed curves) have been obtained by fixing $p_{ass} = 0.45$ and $\tau_{final} = 1$ s at 80 °C, 5 s at 60 °C, 50 s at 40 °C, 250 s at 25 °C and 5000 s at 0 °C.

viscoelastic response of their reference samples. This indicates that the relaxation of the supramolecular chains is dominated by the association dynamics.

We also see that the sample Lin100 k+Cu is relaxing significantly slower than the reference sample (green, ▷), but faster than the corresponding double chains. It is indeed relaxing similarly to the reference sample Lin140 k. We, therefore, expect that the effective association times of the stickers are localized between the relaxation time of the single chains and the relaxation time of the double chains. On the other hand, the influence of the stickers on sample (Lin140 k+Cu) is very weak. Again, this suggests that the lifetimes of the stickers are quite short compared to the relaxation time of sample Lin140 k, and thus the dominating effect, in this case, is the disentanglement of the chain.

We now move on to provide a quantitative account using our modified tube model. Figure 14 compares model predictions and data. The solid lines refer to model predictions when ligand exchange is considered, while dashed lines are the corresponding predictions when sticker dissociation/association events are disregarded. In the latter case, the single and double chains present at time $t = 0$ stay in the same state during the whole frequency range, meaning that they are not allowed to dissociate or associate. This allows us to evaluate the influence of chain dissociation, going from double chains to single chains. Figures 14(a) and 14(c) reveal that at high T the model compares better with the data when ligand exchange is accounted for. Nevertheless, the ligand exchange effect is not as important as in the case of telechelic star molecules in which it is clearly visible. The

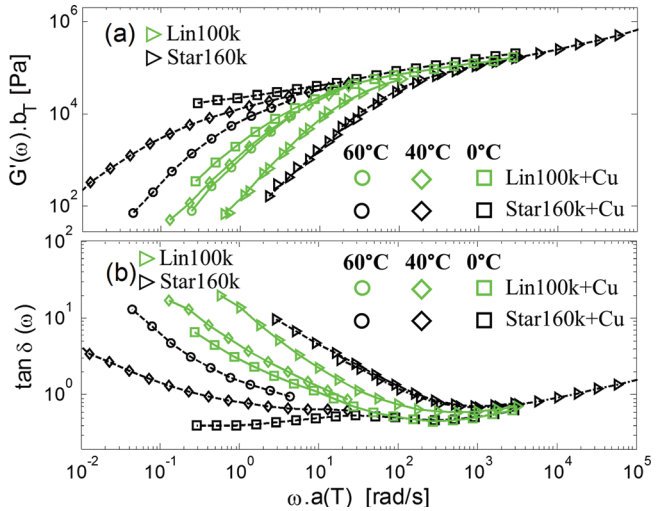

FIG. 12. Storage modulus (a) and tan δ curves (b) of the reference samples Lin100 k (green, ▷) and Star160 k (black, ▷), and of the supramolecular samples Lin100 k+Cu (green) and Star160 k+Cu (black), measured at $T = 60\,^{\circ}$C (○), 40 °C (◇), and 0 °C (□). The data have been shifted to a reference temperature of 25 °C, based on the shift factors determined for the reference samples.

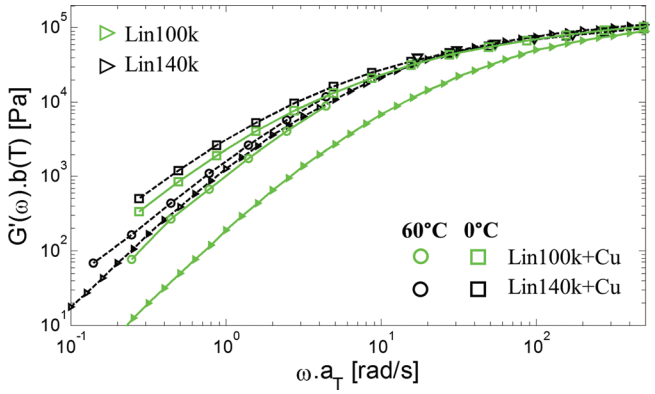

FIG. 13. Storage modulus of the reference samples Lin100 k (green, ▷) and Lin140 k (black, ▷), and of the supramolecular samples Lin100 k+Cu (green) and Lin140 k+Cu (black), measured at $T = 60\,°C$ (○) and $0\,°C$ (□). The data have been shifted to a reference temperature of 25 °C, based on the shift factors determined for the reference samples.

influence of ligand exchange also explains why a well fitted master-curve cannot be constructed with the data of the star complexes at different temperatures. There, the sample relaxation depends on the longest association time τ_{final}, which strongly varies with the temperature, in a different way as the Rouse time of an entanglement segment τ_e. This is further discussed in Sec. IV D.

Interestingly, same values of the longest relaxation time τ_{final}, have been used for all these samples, i.e., for the two linear and the two star polymers, suggesting that the average effective lifetime of an associated bond does not depend on the chain architecture, but is only a function of the temperature. On the other hand, the fraction of associated arms p_{ass}, is found to be identical for the two telechelic stars ($p_{ass} = 0.45$), while it differs for the monofunctional linear chains ($p_{ass} = 0.65$ for Lin100 k and $p_{ass} = 0.25$ for Lin140 k). This can be understood by the fact that these samples have different density of ions and different chain mobility which should affect the ability to create efficient bis-tpy complexes. The low fraction of associated chains of sample (lin140 k+Cu), with an effective association time τ_{final} of 5 s at 60 °C also explains the small influence of the stickers found in Fig. 13 for this sample.

C. Influence of the ion nature

While in Secs. IV A and IV B, the viscoelastic properties of the telechelic molecules in the presence of copper ions have been analyzed, we now vary the nature of the ions. An

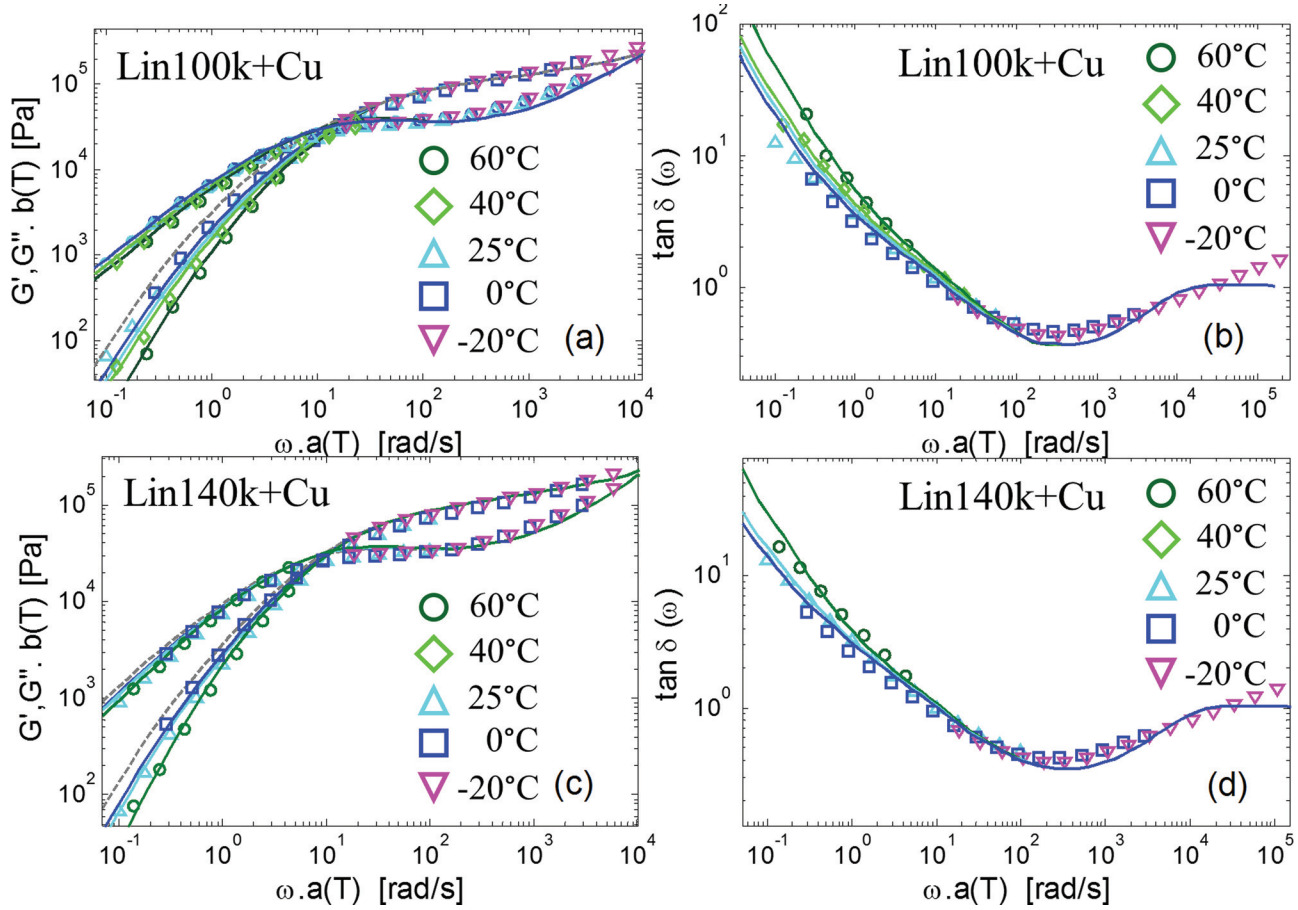

FIG. 14. Storage modulus and Loss modulus and tan δ curves of the mono-functional sample Lin100 k+Cu [panels (a) and (b), respectively] and Lin140 k+Cu [panels (c) and (d), respectively]. The experimental data have been measured at temperature $T = 60\,°C$ (dark green, ○), 40 °C (green, ◇), 25 °C (cyan, Δ), 0 °C (blue, □), and −20 °C (magenta, ▽) and have been shifted to a reference temperature of 25 °C, based on the shift factors determined for the reference samples. The theoretical curves (continuous and dashed curves) have been obtained by fixing $p_{ass} = 0.65$ for Lin100 k+Cu and 0.25 for Lin140 k+Cu, and using the same values of $\tau_{final} = 5$ s at 60 °C, 50 s at 40 °C, 250 s at 25 °C, and 5000 s at 0 °C. The dashed lines represent the predicted moduli if we exclude any sticker dissociation or association.

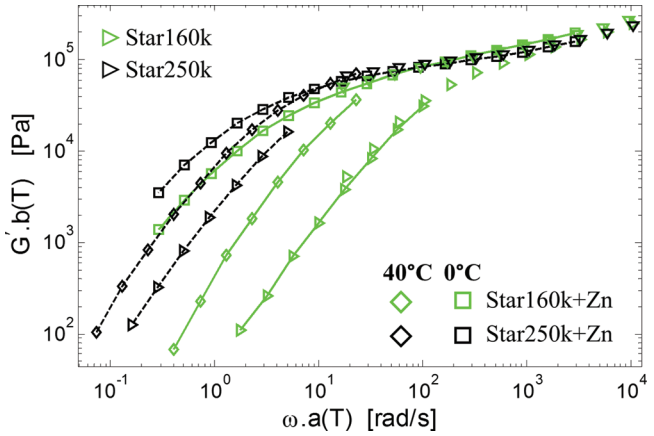

FIG. 15. Storage modulus of the reference samples Star160 k (green, ▷) and Star250 k (black, ▷), and of the supramolecular samples Star160 k+Zn (green) and Star250 k+Zn (black), measured at $T = 40\,^{\circ}\mathrm{C}$ (◇) and $0\,^{\circ}\mathrm{C}$ (□). The data have been shifted to a reference temperature of 25 °C, based on the shift factors determined for the reference samples.

extreme case is found in the star systems associated with zinc ions, which leads to weaker bonds compared to the copper ions [40]. Results obtained with the two star polymers are shown in Fig. 15. Despite the fact that these samples have similar effective association time τ_{final} (see below) and that the associated arms cannot relax before the dissociation of their stickers, it is observed that the two samples have very different terminal times, contrary to the results found with copper (see Fig. 9).

This can be explained by the fact that, in the specific case of Star250 k+Zn, the lifetime of the metallo-supramolecular bonds is relatively short, in comparison to the relaxation time of Star250 k by CLF and arm retraction mechanism. Therefore, their terminal relaxation stays dominated by the disentanglement time and is found to be only slightly longer than the terminal relaxation time of the reference sample (black, ▷) due to slight effect of zinc bis-tpy complexes. On the other hand, the terminal relaxation time of the Star160 k+Zn is longer compared to the relaxation of the Star160 k reference. This indicates that the relaxation of this shorter sample is dominated by the dissociation time, as found with the other ions. In this case, the dissociation time is significantly longer than the relaxation time of the corresponding reference sample. From this example, it is expected that the dissociation time for zinc bis-tpy complex is around 1 s.

Figure 16 below presents a summary of the data based on telechelic samples with zinc ions. Again, same values of the parameter τ_{final} could be used, independently from the chain architecture. Furthermore, the parameter p_{ass} was also found to be the same for these four different sets of associating samples. The low values of the association times are consistent with the fact that the zinc complexes are very labile as

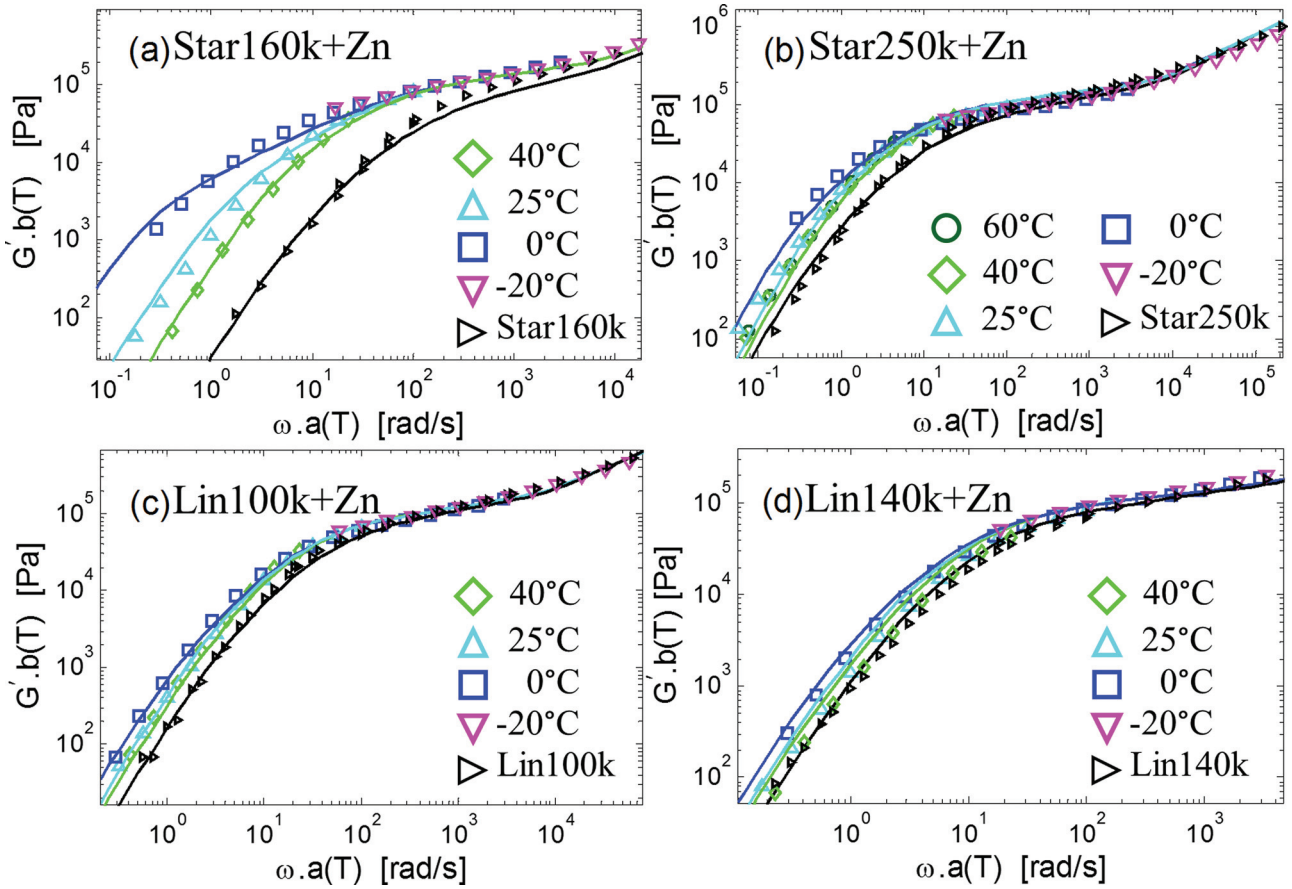

FIG. 16. Storage modulus of samples Star160 k+Zn (a), Star250 k+Zn (b), Lin100 k+Zn (c), and Lin140 k+Zn (d), and their corresponding reference samples (black, ▷). The experimental data have been measured at temperature $T = 60\,^{\circ}\mathrm{C}$ (dark green, ○), $40\,^{\circ}\mathrm{C}$ (green, ◇), $25\,^{\circ}\mathrm{C}$ (cyan, △), $0\,^{\circ}\mathrm{C}$ (blue, □), and $-20\,^{\circ}\mathrm{C}$ (magenta, ▽) and have been shifted to a reference temperature of 25 °C, based on the shift factors determined for the reference samples. The theoretical curves have been obtained by fixing $p_{ass} = 0.4$ for all the samples, as well as $\tau_{final} = 0.07$ s at 60 °C, 0.3 s at 40 °C, 1 s at 25 °C, and 6 s at 0 °C.

discussed earlier. We also see in Fig. 16 that temperature has only a small effect on the terminal relaxation time, compared to the samples with copper ions. This is due to the fact that the contribution of the disentanglement time to the total relaxation time of the molecules [see Eqs. (9) and (10)] becomes important. Therefore, since this part does not depend on temperature, and the data being shifted in the same way as the reference sample, the difference between the different terminal relaxation times is reduced.

On the other hand, if a stronger metal ion is used such as cobalt ions, the thermorheological complexity of the sample is enhanced. This is shown in Fig. 17 for the telechelic Star250 k+Co as well as the two monofunctional linear chains Lin100 k+Co and Lin140 k+Co. Here again, same values of the association time could be used for all these samples. However, a larger discrepancy is observed between the experimental and the theoretical data, especially in the low frequency window of the tan δ curves. In particular, it is observed that a small fraction of sample Lin140 k+Co relaxes slower than the predicted relaxation of linear chains with twice the molecular weight of Lin140 k, i.e., 280 kg/mol [see the dashed curves on Fig. 17(f)]. As discussed in [25], this could be due to the presence of few small aggregates (not detectable by WAXS measurement).

D. Value of the effective association time τ_{final}

Since the theoretical curves have been obtained by determining the longest effective association time τ_{final} by the best fitting procedure, it is interesting to analyze how this

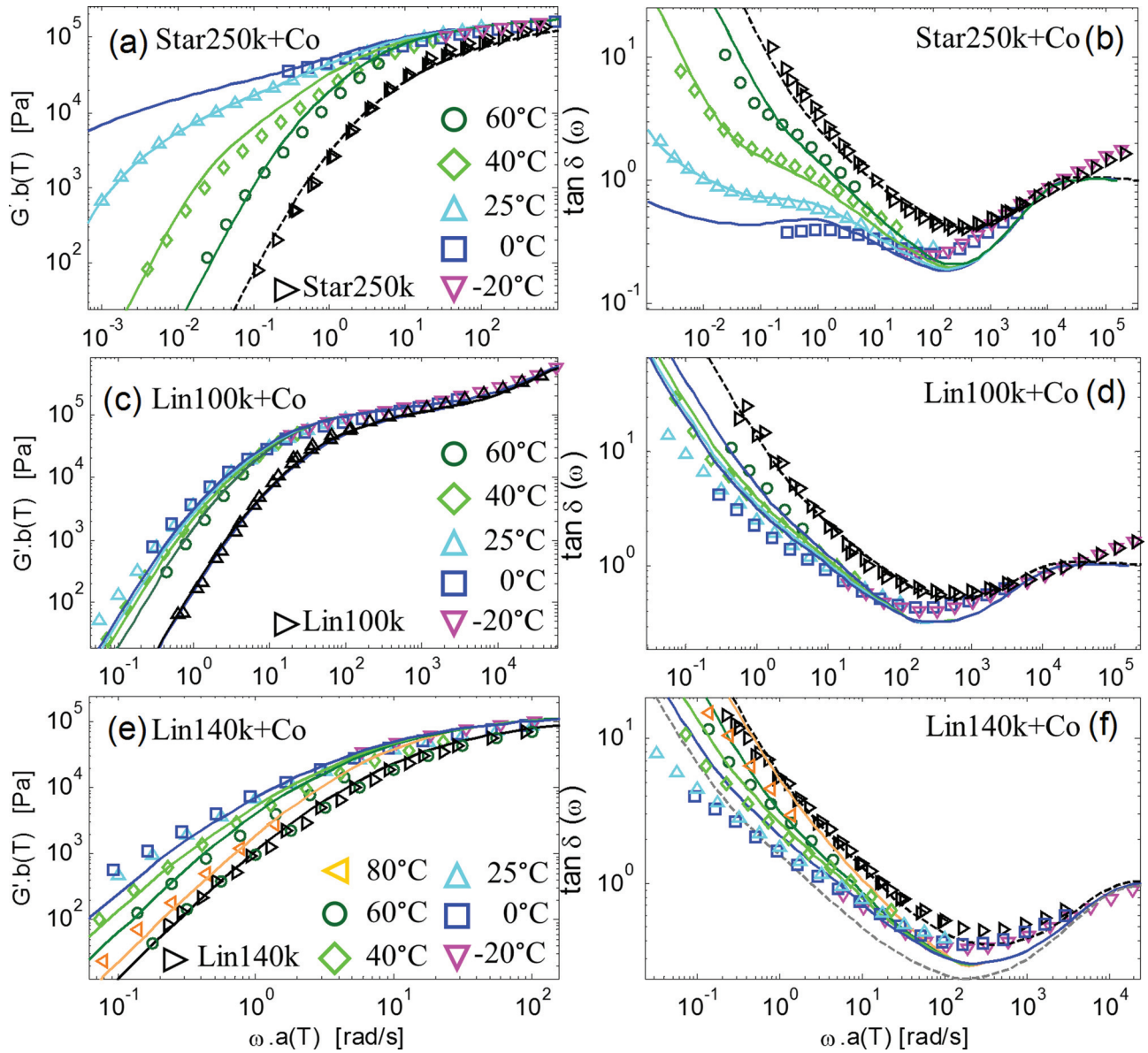

FIG. 17. Storage modulus and tan δ curve of samples Star250 k+Co (a) and (b), Lin100 k+Co (c) and (d) and Lin140 k+Co (e) and (f), and their corresponding reference samples (black, $\triangleright$). The experimental data have been measured at temperature $T = 80\,^{\circ}$C (orange $\triangleleft$), 60 °C (dark green, o), 40 °C (green, $\diamond$), 25 °C (cyan, $\triangle$), 0 °C (blue, $\square$), and $-20\,^{\circ}$C (magenta, $\triangledown$) and have been shifted to a reference temperature of 25 °C, based on the shift factors determined for the reference samples. The theoretical curves have been obtained by fixing $p_{ass} = 0.65$ with the Star250 k and Lin140 k, and $p_{ass} = 0.85$ with the Lin100 k. For all samples, $\tau_{final} = 0.4$ s at 80 °C, 7 s at 60 °C, 70 s at 40 °C, 1200 s at 25 °C, and 4×10^4 s at 0 °C.

parameter depends on temperature for the different ion complexes. The influence of temperature on the local dynamics of the molecules has been taken into account by shifting the experimental data following the WLF equation determined for the reference sample. Therefore, the variation of τ_{final} is only related to the supramolecular dynamics of the reversible bonds. Results are shown in Fig. 18, and we observe that all sets of data fall into a line when plotted in a semi-log graph as a function of the inverse temperature. This is consistent with the Arrhenius dependence, which is known to describe well the temperature dependence of most of the associative systems:

$$\tau_{final}(T) = \tau_{final}(T = 25\,^{\circ}\mathrm{C})\exp\left(\frac{E_a}{RT}\right). \tag{15}$$

This figure clearly shows that the influence of temperature on the dynamics of the reversible bonds follows an Arrhenius equation, while its influence on the local mobility of the molecules is well described by a WLF equation. These two different dependences allow us to explain the thermorheological complexity of the samples. While at high frequency, the relaxation moduli are only governed by the local mobility of the molecules, and thus, follow a WLF equation, the moduli are governed by both dynamics at low frequency. It is also important to note that the experimental terminal relaxation time does not correspond to τ_{final}, but is influenced by both τ_{final} and the disentanglement time of the molecules. Since these two times vary differently with temperature, their relative importance is also a function of T (as shown and discussed with Fig. 9).

From Eq. (15), we can determine the activation energy E_a of the complexes with the different ions. It is found that $E_a = 168$ kJ/mol for Co^{2+}, 125 kJ/mol for Cu^{2+}, and 81 kJ/mol for Zn^{2+}. These relatively high values, especially with cobalt, are consistent with the fact that metal-ligand associations are quite strong associations [41]. Since the effective association time τ_{final}, and thus the activation energy was found not to depend on the chain architecture, one should be able to determine these values for other polymers based on the same tpy-ion complexes. Thus, if τ_{final} can be determined in advance, the only unknown parameter of the model is the average fraction of associated stickers p_{ass}. However, it is important to remind that these results are valid as long as the samples contain a stoichiometric amount of metal ions and that association/dissociation events are achieved via ligand exchanges, as mentioned in Assumption A3. If an excess of ions is considered, the fraction of free dangling ends will be strongly reduced and longer association times will be found (supplementary material) [42].

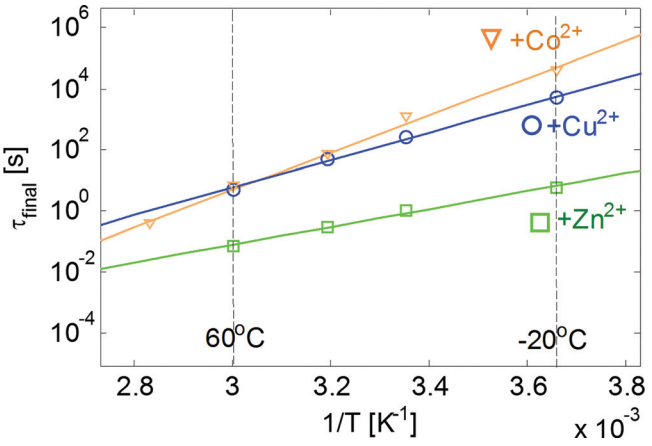

FIG. 18. τ_{final} versus inverse temperature for the systems based on Cu ions (blue ○) or Zn ions (green □) and Co ions (orange ▽).

V. CONCLUSIONS

In this work, we investigated the linear viscoelastic behaviors of entangled telechelic star P*n*BA and monofunctional linear P*n*BA which are able to associate through metal-ligand interactions. tpy was used as ligand and several ions of different lability (Co^{2+}, Cu^{2+}, and Zn^{2+}) were added to the samples, in stoichiometric amount. Based on the experimental data, we could show that the relaxation of the samples depends on both disentanglement and association dynamics. By playing with temperature, we could vary the respective importance of these two processes and analyze their impact on the terminal relaxation time of the samples. It was found that the latter mostly depends on the slower process. By looking at the sample relaxation in the intermediate range of frequency, we also pointed out the presence of a large number of unassociated stickers in the samples.

Based on these observations, we developed a modified version of our tube-based TMA model, in order to account for the dynamics of the stickers. In particular, inspired by the recent work of Wang and coworkers [22], we considered the dissociation of a metal-ligand complex to take place via the ligand exchange. The model contains two unknown parameters, i.e., p_{ass}, the fraction of unassociated stickers, and τ_{final}, the longest time needed to ensure that all the chains were dissociated at least once. We could determine these two parameters by best-fitting procedure and obtain a very good description of the experimental curves. It was found that τ_{final} is not dependent on the chain architecture and is well described by an Arrhenius equation. The corresponding activation energy could be determined, which let the model with only one unknown parameter. Thus, with this work, we now have the necessary framework to explore other metallo-supramolecular networks, based on the different architectures. In particular, we would like to study the viscoelastic behavior of blends of two kinds of telechelic polymers, as well as blends of telechelic and covalent molecules, and to be able to control the modulus of these samples.

ACKNOWLEDGMENTS

This work was financially supported by funding from the People Programme (Marie Curie Actions) of the European Commission's Seventh Framework Programme (FP7/2007-2013) under Supolen REA Grant Agreement No. 607937. E.V.R. and C.A.F. are, respectively, Research Associate and Senior Research Associate of FRS-FNRS. L.G.D.H. thanks Marie Curie Actions for the Post-doctoral research grant. F.Z. thanks Marie Curie Actions for the Ph.D. thesis grant.

NOMENCLATURE

$CoCl_2$	Cobalt chloride (II)
$CuCl_2$	Copper chloride (II)
p_{ass}	Fraction of unassociated stickers at time t
$ZnCl_2$	Zinc chloride (II)
τ_{ass}	Average association time of stickers
τ_e	Entanglement relaxation time
$\tau_{exchange}$	Shorter ligand exchange time
τ_{final}	Longest ligand exchange time
τ_{fluc}	CLF fluctuation time
τ_{rel}	Terminal relaxation time

References

[1] Burattini, S., B. W. Greenland, D. H. Merino, W. Weng, J. Seppala, H. M. Colquhoun, W. Hayes, M. E. MacKay, I. W. Hamley, and S. J. Rowan, "A healable supramolecular polymer blend based on aromatic π-π stacking and hydrogen-bonding interactions," J. Am. Chem. Soc. **132**, 12051–12058 (2010).

[2] Lewis, C. L., K. Stewart, and M. Anthamatten, "The influence of hydrogen bonding side-groups on viscoelastic behavior of linear and network polymers," Macromolecules **47**, 729–740 (2014).

[3] Chen, Q., G. J. Tudryn, and R. H. Colby, "Ionomer dynamics and the sticky Rouse model," J. Rheol. **57**, 1441–1462 (2013).

[4] Chen, Q., H. Masser, H. S. Shiau, S. Liang, J. Runt, P. C. Painter, and R. H. Colby, "Linear viscoelasticity and Fourier transform infrared spectroscopy of polyether-ester-sulfonate copolymer ionomers," Macromolecules **47**, 3635–3644 (2014).

[5] Winter, A., and U. S. Schubert, "Synthesis and characterization of metallo-supramolecular polymers," Chem. Soc. Rev. **45**, 5311–5357 (2016).

[6] Herbst, F., D. Döhler, P. Michael, and W. H. Binder, "Self-healing polymers via supramolecular forces," Macromol. Rapid Commun. **34**, 203–220 (2013).

[7] Cordier, P., F. Tournilhac, C. Soulié-Ziakovic, and L. Leibler, "Self-healing and thermoreversible rubber from supramolecular assembly.," Nature **451**, 977–980 (2008).

[8] Hu, J., Y. Zhu, H. Huang, and J. Lu, "Recent advances in shape-memory polymers: Structure, mechanism, functionality, modeling and applications," Prog. Polym. Sci. **37**, 1720–1763 (2012).

[9] Xie, T., "Tunable polymer multi-shape memory effect," Nature **464**, 267–270 (2010).

[10] Bae, Y., S. Fukushima, A. Harada, and K. Kataoka, "Design of environment-sensitive supramolecular assemblies for intracellular drug delivery: Polymeric micelles that are responsive to intracellular pH change," Angew. Chem. Int. Ed. **42**, 4640–4643 (2003).

[11] Webber, M. J., E. A. Appel, E. W. Meijer, and R. Langer, "Supramolecular biomaterials," Nat. Mater. **15**, 13–26 (2015).

[12] Wei, Q., C. Schlaich, S. Prévost, A. Schulz, C. Böttcher, M. Gradzielski, Z. Qi, R. Haag, and C. A. Schalley, "Supramolecular polymers as surface coatings: Rapid fabrication of healable superhydrophobic and slippery surfaces," Adv. Mater. **26**, 7358–7364 (2014).

[13] Callies, X., C. Véchambre, C. Fonteneau, S. Pensec, Chenal, J.-M., L. Chazeau, L. Bouteiller, G. Ducouret, and C. Creton, "Linear rheology of supramolecular polymers center-functionalized with strong stickers," Macromolecules **48**, 7320–7326 (2015).

[14] Cao, Y., and H. Li, "Polyprotein of GB1 is an ideal artificial elastomeric protein.," Nat. Mater. **6**, 109–114 (2007).

[15] Marrucci, G., S. Bhargava, and S. L. Cooper, "Models of shear-thickening behavior in physically crosslinked networks," Macromolecules **26**, 6483–6488 (1993).

[16] Indei, T., J. D. Schieber, and J. Takimoto, "Effects of fluctuations of cross-linking points on viscoelastic properties of associating polymer networks," Rheol. Acta **51**, 1021–1039 (2012).

[17] Manassero, C., G. Raos, and G. Allegra, "Structure of model telechelic polymer melts by computer simulation," J. Macromol. Sci. Part B Phys. **44**, 855–871 (2005).

[18] Wilson, M., A. Rabinovitch, and A. R. C. Baljon, "Aggregation kinetics of a simulated telechelic polymer," Phys. Rev. E **84**, 061801 (2011).

[19] Rubinstein, M., and A. N. Semenov, "Dynamics of entangled solutions of associating polymers," Macromolecules **34**, 1058–1068 (2001).

[20] Semenov, A. N., and M. Rubinstein, "Dynamics of entangled associating polymers with large aggregates," Macromolecules **35**, 4821–4837 (2002).

[21] Bedrov, D., G. D. Smith, and J. F. Douglas, "Influence of self-assembly on dynamical and viscoelastic properties of telechelic polymer solutions," Europhys. Lett. **59**, 384–390 (2002).

[22] Amin, D., A. E. Likhtman, and Z. Wang, "Dynamics in supramolecular polymer networks formed by associating telechelic chains," Macromolecules **49**, 7510–7524 (2016).

[23] van Ruymbeke, E., D. Vlassopoulos, M. Mierzwa, T. Pakula, D. Charalabidis, M. Pitsikalis, and N. Hadjichristidis, "Rheology and structure of entangled telechelic linear and star polyisoprene melts," Macromolecules **43**, 4401–4411 (2010).

[24] Boudara, V. A. H., and D. J. Read, "Stochastic and preaveraged nonlinear rheology models for entangled telechelic star polymers," J. Rheol. **61**, 339–362 (2017).

[25] Zhuge, F., J. Brassinne, C.-A. Fustin, E. van Ruymbeke, and J.-F. Gohy, "Synthesis and rheology of telechelic entangled bulk metallo-supramolecular polymers," Macromolecules **50**, 5165–5175 (2017).

[26] Jackson, A. C., F. L. Beyer, S. C. Price, B. C. Rinderspacher, and R. H. Lambeth, "Role of metal-ligand bond strength and phase separation on the mechanical properties of metallopolymer films," Macromolecules **46**, 5416–5422 (2013).

[27] Ferry, J. D., *Viscoelastic Properties of Polymers* (Wiley, New York, 1980).

[28] van Ruymbeke, E., E. B. Muliawan, D. Vlassopoulos, H. Gao, and K. Matyjaszewski, "Melt rheology of star polymers with large number of small arms, prepared by crosslinking poly(n-butyl acrylate) macromonomers via ATRP," Eur. Polym. J. **47**, 746–751 (2011).

[29] Walsh, D., P. Zoller, *Standard Pressure-Volume-Temperature Data for Polymers* (CRC, Lancaster, 1995).

[30] Shchetnikava, V., J. J. M. Slot, and E. van Ruymbeke, "A comparison of tube model predictions of the linear viscoelastic behavior of symmetric star polymer melts," Macromolecules **47**, 3350–3361 (2014).

[31] Hawke, L. G. D., M. Ahmadi, H. Gondansaz, and E. van Ruymbeke, "Viscoelastic properties of linear associating poly(n-butyl acrylate) chains," J. Rheol. **60**, 297–310 (2016).

[32] Tierney, N. K., and R. A. Register, "Synthesis and melt dynamics of model sulfonated ionomers," Macromolecules **36**, 1170–1177 (2003).

[33] Chen, Q., Z. Zhang, and R. H. Colby, "Viscoelasticity of entangled random polystyrene ionomers," J. Rheol. **60**, 1031–1040 (2016).

[34] van Ruymbeke, E., D. Vlassopoulos, M. Kapnistos, C. Y. Liu, and C. Bailly, "Proposal to solve the time-stress discrepancy of tube models," Macromolecules **43**, 525–531 (2010).

[35] Ebrahimi, T., H. Taghipour, D. Grießl, P. Mehrkhodavandi, S. G. Hatzikiriakos, and E. van Ruymbeke, "Binary blends of entangled star and linear poly(hydroxybutyrate): Effect of constraint release and dynamic tube dilation," Macromolecules **50**, 2535–2546 (2017).

[36] Taylor, P., and T. C. B. Mcleish, "Tube theory of entangled polymer dynamics," Adv. Phys. **51**, 1379–1527 (2002).

[37] van Ruymbeke, E., V. Shchetnikava, Y. Matsumiya, and H. Watanabe, "Dynamic dilution effect in binary blends of linear polymers with well-separated molecular weights," Macromolecules **47**, 7653–7665 (2014).

[38] Doi, M., and S. F. Edwards, *The Theory of Polymer Dynamics* (Oxford University, New York, 1986).

[39] Milner, S. T., and T. C. B. McLeish, "Parameter-free theory for stress relaxation in star polymer melts," Macromolecules **30**, 2159–2166 (1997).

[40] Holyer, R. H., C. D. Hubbard, S. F. A. Kettle, and R. G. Wilkins, "The kinetics of replacement reactions of complexes of the transition metals with 2,2',2"-terpyridine," Inorg. Chem. **5**, 622–625 (1966).

[41] Mendes, A. C., E. T. Baran, R. L. Reis, and H. S. Azevedo, "Self-assembly in nature: Using the principles of nature to create complex nanobiomaterials," Wiley Interdiscip. Rev. Nanomed. Nanobiotechnol. **5**, 582–612 (2013).

[42] See supplementary material at http://dx.doi.org/10.1122/1.4997593 for SEC of the linear and four-arm star poly(*n*-butyl acrylate)s end-functionalized with terpyridine ligand (P*n*BA-tpy$_x$). UV-vis titration with metal cations of terpyridine end-groups in P*n*BA-tpy$_x$.